Robust topological invariants of topological crystalline phases in the presence of impurities

Ian Mondragon-Shem[1] and Taylor L. Hughes[2]
[1]*Department of Physics, Yale University, New Haven, Connecticut 06520, USA*
[2]*Department of Physics, University of Illinois-Urbana Champaign, Urbana, Illinois 61801, USA*

(Received 1 January 2020; revised 22 October 2023; accepted 1 February 2024; published 18 July 2024)

Topological crystalline phases (TCPs) are topological states protected by spatial symmetries. A broad range of TCPs have been conventionally studied by formulating topological invariants (symmetry indicators) at invariant momenta in the Brillouin zone, which leaves open the question of their stability in the absence of translational invariance. In this work, we show that robust basis-independent topological invariants can be generically constructed for TCPs using projected symmetry operators. Remarkably, we show that the real-space topological markers of these invariants are exponentially localized to the fixed points of the spatial symmetry. As a result, this real-space structure protects them against the presence of impurities that are located away from the fixed points and also sufficiently slowly varying disorder potentials. By considering all possible symmetry centers in a crystalline system we can generate a mesh of real-space topological markers that can provide a local topological distinction for TCPs. We illustrate the robustness of this mesh of invariants with one- and two-dimensional TCPs protected by inversion, rotational, and mirror symmetries. Finally, we find that the boundary modes of these TCPs can also exhibit robust topological invariants with localized markers on the edges. We illustrate this with the gapless Majorana boundary modes of mirror-symmetric topological superconductors, and relate their integer topological edge invariant with a quantized effective edge polarization.

DOI: 10.1103/PhysRevB.110.035146

I. INTRODUCTION

Over the past decade, dramatic progress has been made in understanding the interplay between symmetry and topology in quantum phases of matter [1,2]. A particular focus has been the so-called topological crystalline phases (TCP) [3,4], which are topological states protected by spatial symmetries. A number of experiments have already revealed their existence in nature [5–8], and over the course of just a few years, significant theoretical progress has been made [9–27].

It has been argued that the surface states of TCPs are robust to the presence of disorder as long as it is symmetric on average [28–30]. Experimental signatures of TCPs appear to be qualitatively consistent with this idea, even in crystals that are expected to have moderate amounts of disorder from alloying, e.g., $Pb_xSn_{1-x}Te$ [31]. Bulk studies have also argued the existence of statistical topological insulators which have protected boundary modes as long as the spatial symmetry is preserved on average [29,30,32]. Notwithstanding these studies, a bulk understanding of the mechanism behind the robustness of TCPs against the presence of impurities is still lacking, especially in cases in which a notion of average symmetry has not been clearly defined.

In this work, we find that a large class of TCPs protected by point-group symmetries can be characterized by a mesh of topological invariants that can be robustly quantized even in the presence of impurities. To demonstrate this we construct basis-independent forms of topological invariants protected by point-group symmetry, and show that their associated position-space topological markers are *spatially localized* to the fixed points of the spatial symmetry. We then construct a mesh of such invariants by considering invariants defined on each of the symmetry centers of the lattice. We provide evidence that this mesh can remain robust in the presence of impurities, and can provide some rigidity to the TCP. We exemplify our results for one-dimensional (1D) inversion-symmetric insulators, two-dimensional (2D) rotation-symmetric superconductors, and 2D mirror-symmetric superconductors. In the latter case, we also find cases in which the edge states are also characterized by topological invariants that are themselves robustly quantized in the presence of impurities.

II. LOCALIZED MARKERS IN 1D INVERSION-SYMMETRIC INSULATORS

We begin by analyzing 1D topological insulators protected by inversion symmetry on a lattice having an even number of sites L_x. On a system with periodic boundary conditions and lattice translation symmetry, there is an extensive set of possible inversion-symmetry operations $P_{\mathcal{S}}$ distinguished by the two positions $\mathcal{S} = \{R_1 + r_0, R_2 + r_0\}$ they leave invariant; here, $R_{1,2}$ each label a unit cell, and r_0 takes one of two possible values 0 or $\frac{1}{2}$. For this work, we focus on gapped Hamiltonians $\hat{H}$ such that $[\hat{p}_{\mathcal{S}}, \hat{H}] = 0$, where $\hat{p}_{\mathcal{S}}$ is the Hilbert space representation of $P_{\mathcal{S}}$.

The conventional topological classification of inversion-symmetric insulators implicitly assumes translation symmetry and proceeds by formulating the problem with a Bloch Hamiltonian in momentum space $\hat{H} = \sum_{k_x} c^{\dagger}_{k_x} h(k_x) c_{k_x}$. The Bloch Hamiltonian must satisfy $\widetilde{p}_{\mathcal{S}}(k_x) h(k_x) \widetilde{p}^{-1}_{\mathcal{S}}(k_x) = h(P_{\mathcal{S}} k_x)$, where $\widetilde{p}_{\mathcal{S}}(k_x)$ is the momentum representation of the inversion operator. At the inversion-invariant momenta

$k_x^{\rm inv} = 0, \pi$, the Bloch states can be labeled with inversion eigenvalues. Let $n_{\mathcal{S}}^{(\pm)}(k_x^{\rm inv})$ denote the number of occupied states with inversion eigenvalues ± 1 at momentum $k_x^{\rm inv}$, and let us define

$$\Delta_{\mathcal{S}}^{p} = \sum_{k_x^{\rm inv}} \left[n_{\mathcal{S}}^{(+)}(k_x^{\rm inv}) - n_{\mathcal{S}}^{(-)}(k_x^{\rm inv}) \right]. \tag{1}$$

It was shown in [33] that $\Delta_{\mathcal{S}}^{p}|_{r_0=1/2}$ is an integer invariant that distinguishes 1D inversion-symmetric topological insulators from the trivial atomic limit. For example, a simple model with nontrivial $\Delta_{\mathcal{S}}^{p}|_{r_0=1/2}$ is $h(k_x) = \sin k_x \sigma_2 + (m - \cos k_x)\sigma_1$, where the σ_a are Pauli matrices acting on two orbitals $\{A, B\}$ per cell. The inversion operator is $\tilde{p}_{\mathcal{S}}(k_x^{\rm inv}) = e^{-2ik_x^{\rm inv} r_0}\sigma_1$, which leads to $\Delta_{\mathcal{S}}^{p}|_{r_0=1/2} = 2(0)$ in the topological (trivial) phase.

As it stands, the computation of $\Delta_{\mathcal{S}}^{p}$ relies on momentum being a good quantum number. It is thus unclear to what extent $\Delta_{\mathcal{S}}^{p}$ can remain quantized when translation symmetry is broken by disorder. However, even with translation symmetry, using the momentum-space description is just a choice of basis. Hence, we expect there is a way to compute the topological invariant in a basis-independent manner. Indeed, we find that we can write $\Delta_{\mathcal{S}}^{p}$ in the general form (see Appendix)

$$\Delta_{\mathcal{S}}^{p} = \mathrm{Tr}[\bar{p}_{\mathcal{S}}], \tag{2}$$

where $\bar{p}_{\mathcal{S}} = \mathcal{P}_G \hat{p}_{\mathcal{S}} \mathcal{P}_G$, and $\mathcal{P}_G = \sum_{n\in \rm occ.} |u_n\rangle\langle u_n|$ is the projector onto the occupied single-particle states. Thus, instead of analyzing the contributions to $\Delta_{\mathcal{S}}^{p}$ in momentum space, Eq. (2) affords us a way to study its position-space structure by taking the trace in the position basis.

To this end, it is natural to consider the spatially resolved topological marker

$$\mathcal{T}_{\mathcal{S}}^{p}(x) = \langle x|\mathrm{Tr}_{\circ}[\bar{p}_{\mathcal{S}}]|x\rangle, \tag{3}$$

where $\mathrm{Tr}_{\circ}$ traces over only the local degrees of freedom in each unit cell. The topological invariant is thus given by $\Delta_{\mathcal{S}}^{p} = \sum_{x=1}^{L_x} \mathcal{T}_{\mathcal{S}}^{p}(x)$. Topological markers have been used in other contexts to study the local properties of topological phases [34–38]. Remarkably, we can identify a generic structure in the topological markers of gapped systems by noting (i) the position matrix elements for the inversion operator satisfy $\langle x, \alpha|\hat{p}_{\mathcal{S}}|x', \beta\rangle \propto \delta_{x,\mathcal{P}_{\mathcal{S}}x'}$, and (ii) for a gapped or localized system with inverse gap or localization length of order ζ, the position matrix elements of the projector satisfy $|\langle x', \alpha|\mathcal{P}_G|x, \beta\rangle| < O(e^{-|x-x'|/\zeta})$ when $|x - x'| \gg \zeta$. Using these results, the topological marker obeys

$$\left|\mathcal{T}_{\mathcal{S}}^{p}(x)\right| < O(e^{-2|x-\mathcal{S}|/\zeta}) \quad \text{for } |x - \mathcal{S}| \gg \zeta, \tag{4}$$

where $|x - \mathcal{S}|$ denotes the smallest distance of x to any of the fixed points in $\mathcal{S}$. Hence, Eq. (4) implies that, for a given $P_{\mathcal{S}}$, the associated topological marker is localized in a neighborhood of $\mathcal{S}$. We illustrate one of these localized markers in Fig. 1(a); the inset shows the marker on a logarithmic scale to confirm its exponential localization.

We note that this stands in sharp contrast to the topological markers of Chern insulators and other strong topological insulators, which have markers that are *not* spatially localized. The spatial symmetry, combined with the exponential decay of the projector for a gapped or localized system produces the spatial localization. Interestingly, the full set of operators $P_{\mathcal{S}}$ for a translationally invariant lattice generates a position-space mesh of localized topological markers, and their associated invariants, that are spread throughout the lattice [cf. red dots in Figs. 1(c)–1(e)]. This mesh, which we will define more precisely below, endows topological crystalline phases with some local robustness against impurities as we now discuss.

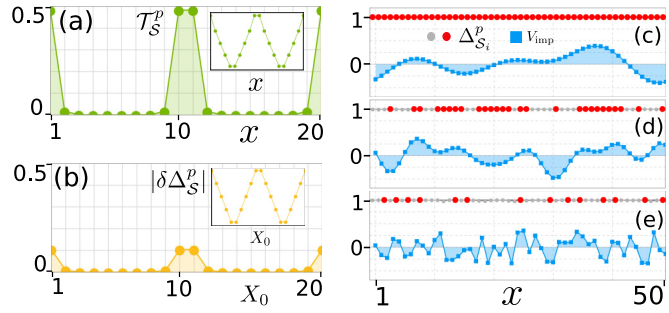

FIG. 1. Inversion-symmetric 1D insulator. (a) Topological marker $\mathcal{T}_{\mathcal{S}}^{p}(x)$. The inset shows the same data on a logarithmic scale. (b) Deviation of the invariant $|\delta\Delta_{\mathcal{S}}^{p}|$ induced by an impurity at position X_0. The inset shows the same data on a logarithmic scale. (c)–(e) The net local invariant $\Delta_{\mathcal{S}_i}^{p}$ (red and gray dots) for each inversion center $\mathcal{S}$ as the distribution of impurities (blue squares) increases its spatial variation. The dots that are red denote the cases for which $|\Delta_{\mathcal{S}_i}^{p}|$ differs from the clean-limit value 1.0 by 10^{-3}, whereas gray dots deviate more significantly.

Suppose we add an impurity at a position X_0, where for our purposes an impurity is any localized term in the Hamiltonian, which of course breaks translational symmetry. The projection operator of the new ground state in the presence of the impurity can be written as $\mathcal{P}'_G = \mathcal{P}_G + \delta\mathcal{P}_G$. Since the system is gapped, $\delta\mathcal{P}_G$ has support in an exponentially small neighborhood of size ζ centered at the impurity. For an impurity placed far away from $\mathcal{S}$, and using $\langle x|\delta\mathcal{P}_G|X_0\rangle < O(e^{-|X_0-x|/\zeta})$, we find the basis-independent expression

$$\left|\delta\Delta_{\mathcal{S}}^{p}\right| \equiv \left|\Delta_{\mathcal{S}}^{p'}(X_0) - \Delta_{\mathcal{S}}^{p}\right| < O(e^{-2|X_0-\mathcal{S}|/\zeta}). \tag{5}$$

This implies that the effect of the impurity on $\Delta_{\mathcal{S}}^{p}$ is exponentially suppressed in the distance between the impurity center and the inversion center(s). We confirm this numerically in Fig. 1(b) where we show $|\delta\Delta_{\mathcal{S}}^{p}|$ as a function of the impurity position X_0. This effect holds even if the impurity strength is much greater than the bulk energy gap since the topology is encoded in a localized manner. Furthermore, we can define a mesh of topological invariants by summing each topological marker over the neighborhood of *one* inversion center: $\Delta_{\mathcal{S}_i}^{p} = \sum_{|x-\mathcal{S}_i|<\zeta} \mathcal{T}_{\mathcal{S}}^{p}(x)$, such that $\Delta_{\mathcal{S}}^{p} \approx \sum_{i=1,2} \Delta_{\mathcal{S}_i}^{p}$ (i runs over the two invariant points in $\mathcal{S}$). For our example model, in the topological phase and without impurities, we have $\Delta_{\mathcal{S}_i}^{p}|_{r_0=1/2} = 1$, and hence $\Delta_{\mathcal{S}}^{p}|_{r_0=1/2} = 2$. Our results for a single impurity imply that if we consider the full mesh of invariants, only those exponentially close to the impurity have a chance to be strongly impacted, hence, the mesh of topological invariants is robust.

While we have argued that local invariants away from an impurity remain robust, we will now show that the invariants can remain robust even when impurities are close to the their

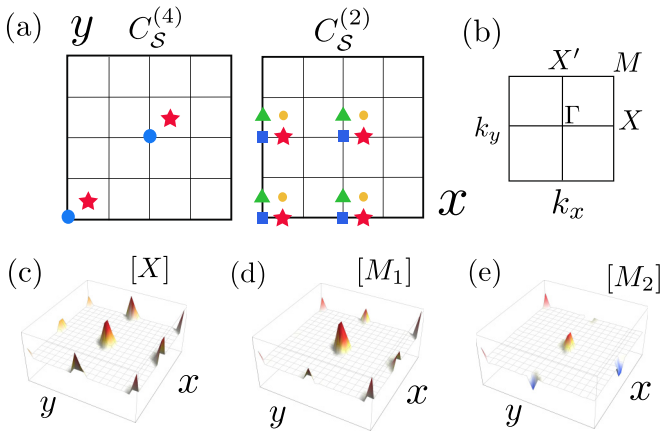

FIG. 2. Rotationally symmetric 2D superconductors. (a) Invariant points under $C_S^{(4)}$ (left) and $C_S^{(2)}$ (right). For example, in the former case, each set of symbols maps to themselves under fourfold rotations centered at that symbol. (b) Invariant momenta in the BZ. (c)–(e) Topological markers for the rotationally symmetric topological superconductor with $(\mathrm{Ch}, [X], [M_1], [M_2]) = (1, 1, 1, 0)$.

associated symmetry center. To show this, instead of a single impurity let us focus on a disorder potential $V(r)$. We expect that if $V(r)$ varies on a scale ξ, the TCP should remain robust as long as $\zeta \ll \xi$. This will effectively lead to a locally inversion-symmetric system, even though the Hamiltonian does not commute with the inversion operator. In Figs. 1(c)–1(e) we show the mesh of invariants $\Delta^p_{\mathcal{S}_i}$ for all possible $\mathcal{S}$ as the impurity potential progressively varies more rapidly in space. When the potential varies slowly [Fig. 1(c)], *all* invariants remain robustly quantized. As the potential is made to vary more rapidly, the impurities destroy the quantization of the mesh at some points (gray dots), while at other regions $\Delta^p_{\mathcal{S}_i}$ remains robustly quantized (red dots). Thus, the system can retain a local distinction between the trivial and nontrivial topological phases (i.e., unobstructed and obstructed atomic limits). Interestingly, even in the worst-case scenario of completely uncorrelated disorder [Fig. 1(e)], some invariants in the mesh remain robustly quantized.

Let us also note that the strength of the potential can have an impact on the topological mesh. We expect that a slowly varying potential preserves the quantization of the local invariants unless it is strong enough to close the gap or mix localized states with delocalized states at that point. However, we expect that a potential that locally varies faster than ζ, say on the scale of the lattice, can destroy the quantization even for weaker strengths without the gap closing.

III. LOCALIZED MARKERS IN 2D ROTATION-SYMMETRIC SUPERCONDUCTORS

Next, we consider 2D topological superconductors protected by rotation symmetries and without time-reversal symmetry. With periodic boundary conditions, a given n-fold rotation operation $C_S^{(n)}$ leaves invariant a set of positions $\mathcal{S} = \{\mathbf{R}_i + \mathbf{r}_0\}$ [see Fig. 2(a)]. Defining $2\mathbf{a}_1$ and $2\mathbf{a}_2$ as primitive vectors, then $\mathbf{r}_0 \in \{\mathbf{0}, \mathbf{a}_1 + \mathbf{a}_2\}$ for $C_S^{(4)}$, whereas $\mathbf{r}_0 \in \{\mathbf{0}, \mathbf{a}_1, \mathbf{a}_2, \mathbf{a}_1 + \mathbf{a}_2\}$ for $C_S^{(2)}$. We consider models that satisfy $[\hat{c}_S^{(n=2,4)}, \hat{H}] = 0$, where $\hat{c}_S^{(n)}$ is the representation of $C_S^{(n)}$. The conventional classification of rotation-symmetric insulators focuses on Bloch states at the rotation-invariant momenta which can be labeled by rotation eigenvalues. As illustrated in Fig. 2(b), $\hat{c}_S^{(n=4)}$ ($\hat{c}_S^{(n=2)}$) leaves invariant the momenta Γ, M (Γ, M, X, X'). One of the topological invariants in this symmetry class is a Chern number Ch, which exists regardless of the spatial symmetries. Additionally, there are three more integers ($[X]$, $[M_1]$, $[M_2]$) [15,16]. These invariants count the difference in the number of occupied states at the X, M points that have rotation eigenvalues $(e^{i\pi/2}, e^{i\pi/4}, e^{i3\pi/4})$, respectively, compared to those at Γ.

Rather than writing out momentum-space expressions for these invariants, we can again express them in a basis-independent manner. By defining the projected rotation operators $\bar{c}_S^{(n)} = \mathcal{P}_G \hat{c}_S^{(n)} \mathcal{P}_G$, we obtain (see Appendix)

$$[X] = \frac{i}{4}\mathrm{Tr}\left[\left(\bar{c}_S^{(2)}\big|_{\mathbf{r}_0=\mathbf{a}_1}\right) + \left(\bar{c}_S^{(2)}\big|_{\mathbf{r}_0=\mathbf{a}_1+\mathbf{a}_2}\right)\right], \tag{6}$$

$$[M_{1,2}] = \frac{i}{4}\mathrm{Tr}\left[\sqrt{2}\left(\bar{c}_S^{(4)}\big|_{\mathbf{r}_0=\mathbf{a}_1+\mathbf{a}_2}\right) \pm \left(\bar{c}_S^{(2)}\big|_{\mathbf{r}_0=\mathbf{a}_1}\right)\right]. \tag{7}$$

Similarly to the inversion-symmetric case, the presence of $\bar{c}_S^{(n)}$ in these expressions implies that these invariants have exponentially localized topological markers. To exemplify the topological markers associated with these invariants, let us consider the following model:

$$\begin{aligned} h(\mathbf{k}) = {} & \sin(\mathbf{k}\cdot\mathbf{a}_1)\tau_1 + \sin(\mathbf{k}\cdot\mathbf{a}_2)\tau_2 \\ & + u_1[\cos(\mathbf{k}\cdot\mathbf{a}_1) + \cos(\mathbf{k}\cdot\mathbf{a}_2)]\tau_3 \\ & + u_2[\cos(\mathbf{k}\cdot\mathbf{a}_1') + \cos(\mathbf{k}\cdot\mathbf{a}_2')]\tau_3, \end{aligned} \tag{8}$$

where $\mathbf{a}_1 = a(1, 0)$, $\mathbf{a}_2 = a(0, 1)$, $\mathbf{a}_1' = \mathbf{a}_1 + \mathbf{a}_2$, and $\mathbf{a}_1' = -\mathbf{a}_1 + \mathbf{a}_2$, a is the lattice constant, and the Pauli matrices τ_a act on the Nambu degree of freedom. We choose $u_1 = 1.0$ and $u_2 = 0.5$, which leads to $(\mathrm{Ch}, [X], [M_1], [M_2]) = (1, 1, 1, 0)$. The corresponding topological markers are illustrated in Figs. 2(c)–2(e), which indeed are spatially localized to the symmetry centers. As with the previous 1D case, this localization can be used to define a local mesh of invariants that grants these TCPs robustness against the addition of impurities.

IV. GENERAL ROBUST TOPOLOGICAL INVARIANTS OF TCPS

Our results suggest that many TCPs should support a robust mesh of localized topological markers. Naively, one might have attempted a systematic study of such robust invariants in terms of exponentially localized Wannier functions. But, interestingly, the rotational case above shows that such topological markers are still localized even when $\mathrm{Ch} \neq 0$, which precludes the construction of localized Wannier functions. The localized nature of topological markers is thus more general, being fundamentally due to the action of projected symmetry operators of gapped or localized systems.

We now show that robust invariants can indeed be constructed using projected symmetry operators for a large class of TCPs that are invariant under a spatial symmetry $\hat{g}_S$, where again $\mathcal{S}$ labels a choice of symmetry center(s). Consider a Bloch Hamiltonian $h(\mathbf{k}_G)$ of a d-dimensional system obtained

by Fourier transforming *only* the spatial components $\mathbf{r}_G$ that change under $G_{\mathcal{S}}$; we denote by $d_G(\leqslant d)$ the number of components of $\mathbf{r}_G$. For example, under C_4^z symmetry only the x and y components change, hence, $\mathbf{r}_G = (x, y)$, $d = 2$ or 3, and $d_G = 2$. At the invariant momenta in the BZ dual to $\mathbf{r}_G$, the states $\{|u^n_{j\mathbf{k}_G^{\rm inv}}\rangle\}$ are labeled by the eigenvalues $\{e^{i\phi_j(\mathbf{k}_G^{\rm inv})}\}$ of $\widetilde{g}_{\mathcal{S}}(\mathbf{k}_G^{\rm inv})$ where j runs over the set of symmetry representations, and n is a band index.

The topological invariants (e.g., symmetry indicators, mirror Chern numbers) of a large class of TCPs are conventionally obtained using projection operators at $\mathbf{k}_G^{\rm inv}$: $\mathcal{P}_{j\mathbf{k}_G^{\rm inv}} = \sum_{n\in \rm occ.} |u^n_{j\mathbf{k}_G^{\rm inv}}\rangle\langle u^n_{j\mathbf{k}_G^{\rm inv}}|$. Let us generally denote such topological invariants as $\tau_j(\mathbf{k}_G^{\rm inv})$. Examples include the counting of states with a particular symmetry eigenvalue, or for instance mirror-winding numbers and mirror-Chern numbers [3,12]. In all of these examples, one finds that $\tau_j(\mathbf{k}_G^{\rm inv}) = {\rm Tr}[\mathcal{F}(\mathcal{P}_{j\mathbf{k}_G^{\rm inv}})]$, where $\mathcal{F}$ is a suitably defined function of $\mathcal{P}_{j\mathbf{k}_G^{\rm inv}}$ that ultimately projects the trace into a sum over occupied states. For example, in the simplest case of counting occupied symmetry representations we just have $\mathcal{F}(\mathcal{P}_{j\mathbf{k}_G^{\rm inv}}) \propto \mathcal{P}_{j\mathbf{k}_G^{\rm inv}}$. More generally, $\mathcal{F}(\mathcal{P}_{j\mathbf{k}_G^{\rm inv}})$ could also involve commutators of $\mathcal{P}_{j\mathbf{k}_G^{\rm inv}}$ with position operators that are *not* components of $\mathbf{r}_G$. Examples include mirror ($y \to -y$) winding numbers for which $\mathcal{F}(\mathcal{P}_{jk_y^{\rm inv}}) \propto \mathcal{P}_{jk_y^{\rm inv}}[\hat{X}, \mathcal{P}_{jk_y^{\rm inv}}]$ where $(d = 2, d_G = 1)$; and mirror ($z \to -z$) Chern invariants for which $\mathcal{F}(\mathcal{P}_{jk_z^{\rm inv}}) \propto \mathcal{P}_{jk_z^{\rm inv}}[[\hat{X}, \mathcal{P}_{jk_z^{\rm inv}}], [\hat{Y}, \mathcal{P}_{jk_z^{\rm inv}}]]$ where $(d = 3, d_G = 1)$.

Now, the $\tau_j(\mathbf{k}_G^{\rm inv})$ are clearly not robust to the presence of impurities since they depend on identifying well-defined momenta in the BZ. We can nevertheless construct new robust invariants through the remarkably simple linear combination

$$T^g_{\mathcal{S}} \equiv \sum_{j,\mathbf{k}_G^{\rm inv}} e^{i\phi_j(\mathbf{k}_G^{\rm inv})}\tau_j\big(\mathbf{k}_G^{\rm inv}\big). \tag{9}$$

The robustness of the $T^g_{\mathcal{S}}$ is made manifest when we rewrite them in terms of a trace over the full Hilbert space, leading to the basis-independent expression

$$T^g_{\mathcal{S}} = {\rm Tr}[\overline{g}_{\mathcal{S}}\mathcal{F}(\mathcal{P}_{\rm G})], \tag{10}$$

which we derive in the Appendix, with $\overline{g}_{\mathcal{S}} = \mathcal{P}_G\hat{g}_{\mathcal{S}}\mathcal{P}_G$ and $\mathcal{P}_G = \sum_{j\mathbf{k}_G}\mathcal{P}_{j\mathbf{k}_G}$. Since the invariants depend on $\overline{g}_{\mathcal{S}}$, we thus find that their topological markers are localized as a function of $\mathbf{r}_G$:

$$\big|\mathcal{T}^g_{\mathcal{S}}(\mathbf{r}_G)\big| < O(e^{-|G_{\mathcal{S}}\mathbf{r}_G - \mathbf{r}_G|/\zeta}) \quad \text{for} \quad \zeta \ll |G_{\mathcal{S}}\mathbf{r}_G - \mathbf{r}_G|. \tag{11}$$

As an immediate consequence, if we place an impurity at $\mathbf{R}_0$ far from $\mathcal{S}$, then [cf. Eq. (5)]

$$\big|T^{g'}_{\mathcal{S}}(\mathbf{R}_0) - T^g_{\mathcal{S}}\big| < O(e^{-|G_{\mathcal{S}}\mathbf{R}_0 - \mathbf{R}_0|/\zeta}). \tag{12}$$

We thus see that the topology of these TCPs is generically encoded in localized meshes of topological markers that are robust against the presence of impurities. These localized markers are consistent with other real-space layered approaches [22,39,40], as well as with approaches using path-integral formulations [41–43], though the focus of these works was not on the effects of disorder.

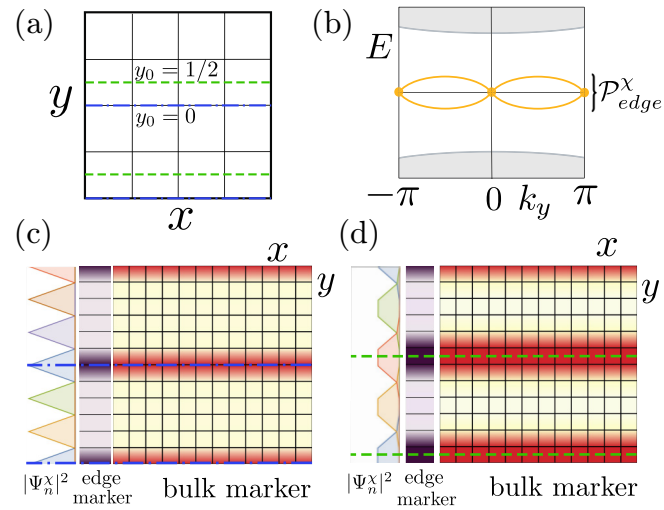

FIG. 3. Mirror-symmetric DIII 2D superconductor. (a) Mirror-invariant lines at $y_0 = 0$ (dashed-dotted blue) and $y_0 = \frac{1}{2}$ (dashed green). (b) Schematic of the energy bands in the BZ for TCPs with trivial DIII strong index. (c), (d) Topological markers of the bulk (square lattice) and edge (purple strip) invariants, as well as some of the Wannier functions $|\Psi^{\chi}_n|^2$ at the edge for the phases (ii) and (iii) discussed in the main text.

V. ROBUST TOPOLOGICAL MARKERS AT THE BOUNDARY

After completing our discussion on general bulk topological markers for TCPs, we now demonstrate that the boundary modes of TCPs can also exhibit robust topological markers connected with the localized bulk invariants $T^g_{\mathcal{S}}$. To exemplify this, consider 2D mirror-symmetric superconductors in class DIII [12]. This symmetry class is described by a Bogoliubov–de Gennes Hamiltonian $h(k_y)$ that commutes with a mirror operator $\hat{m}_{\mathcal{S}}$ that sends $y \to -y$, and where $\mathcal{S} = (Y_1 + y_0, Y_2 + y_0)$ denotes the mirror-invariant lines [see Fig. 3(a)]; we assume $\hat{m}^2_{\mathcal{S}} = -1$. A chiral symmetry $\hat{\chi} = TC$ arises from having both time-reversal T and particle-hole C symmetries, and satisfies $\{T, \hat{\chi}\} = 0$. Chiral symmetry implies that, in the basis in which $\hat{m}_{\mathcal{S}}$ is diagonal, each mirror block of $h(k_y^{\rm inv})$ belongs to class AIII [12]. Hence, a natural topological invariant to apply is the basis-independent topological winding number of class AIII [44]. Indeed, each mirror block has a topological winding invariant

$$\nu^{\pm}_{\mathcal{S}}\big(k_y^{\rm inv}\big) = {\rm Tr}[\mathcal{F}(\mathcal{P}_{\pm,k_y^{\rm inv}})], \tag{13}$$

where

$$\mathcal{F}(\mathcal{P}_{\pm,k_y^{\rm inv}}) = 2L_x^{-1}\mathcal{P}_{\pm,k_y^{\rm inv}}[\hat{X}, \mathcal{P}_{\pm,k_y^{\rm inv}}]\hat{\chi}, \tag{14}$$

and $\hat{X}$ is the position operator. By implementing Eq. (9), we obtain the robust (bulk) invariant

$$T^m_{\mathcal{S}} = {\rm Tr}[\overline{m}_{\mathcal{S}}\mathcal{F}(\mathcal{P}_G)]. \tag{15}$$

In what follows, we use the invariant $\mathcal{V}^m_{\mathcal{S}} = -\frac{i}{2}T^m_{\mathcal{S}}$, with an added prefactor to simplify later expressions.

As expected, the presence of the projected mirror operator $\overline{m}_{\mathcal{S}}$ in the expression for $\mathcal{V}^m_{\mathcal{S}}$ localizes these integer-valued, position-space topological markers to mirror lines. Let us consider three representative cases. (i) If $\mathcal{V}^m_{\mathcal{S}}|_{y_0=0} = \mathcal{V}^m_{\mathcal{S}}|_{y_0=1/2} = 1$,

then the full mesh of markers is nonvanishing and has support on every possible mirror line of the lattice. This implies a nontrivial (strong) DIII $\mathbb{Z}_2$ index, and a single Kramers' pair of propagating helical Majorana modes at the boundary. (ii) If $\mathcal{V}^m_{\mathcal{S}}|_{y_0=0} \neq 0$ and $\mathcal{V}^m_{\mathcal{S}}|_{y_0=1/2} = 0$, then nonvanishing markers are centered at $y_0 = 0$. Such a phase has a trivial DIII $\mathbb{Z}_2$ index, and is adiabatically connected to the limit of decoupled DIII mirror-symmetric wires parallel to the x axis and stacked in the y direction; as such it is a weak topological superconductor. (iii) If $\mathcal{V}^m_{\mathcal{S}}|_{y_0=0} = 0$ and $\mathcal{V}^m_{\mathcal{S}}|_{y_0=1/2} \neq 0$, then its DIII strong invariant is trivial, but it has nontrivial markers that are localized on y lines centered halfway between cells. Thus, while this is still adiabatically connected to a decoupled wire limit, the wires are shifted by half a unit cell in the y direction compared to case (ii). This case is unusual and has a quantized edge topological invariant we will discuss below. To exemplify cases (ii) and (iii), let us consider the Hamiltonian

$$h(\mathbf{k}) = \sin k_x \Gamma_1 + t_y \sin k_y (\Gamma_2 + m_3 \Lambda_3) + (\mu + \cos k_x + t_y \cos k_y)\Gamma_3 + \sum_{i=1}^{2} m_i \Lambda_i, \quad (16)$$

where $\Gamma_1 = f_3\tau_3\sigma_3$, $\Gamma_2 = f_0\tau_3\sigma_1$, $\Gamma_3 = f_0\tau_1\sigma_0$, $\Lambda_1 = f_3\tau_1\sigma_0$, $\Lambda_2 = f_2\tau_1\sigma_3\Lambda_3 = f_1\tau_3\sigma_2$. Here, the Pauli matrices τ_a, σ_a, f_a act on Nambu, spin, and orbital degrees of freedom, respectively. The time-reversal, charge-conjugation, chiral, and mirror operators are $T = \sigma_2 K$, $C = i\tau_2\sigma_2 K$, $S = \tau_2$, and $\widetilde{m}_{\mathcal{S}}(k_y) = ie^{2ik_y y_0}\sigma_3$, respectively. The parameters we choose are indicated in the table below:

	t_y	μ	m_1	m_2	m_3
Weak TCP	0.25	−1.0	1.0	0.0	0.0
Mirror TCP	1.0	0.0	−1.0	0.5	0.5

These parameter values realize a weak TCP with $(\mathcal{V}^m_{\mathcal{S}}|_{y_0=0}, \mathcal{V}^m_{\mathcal{S}}|_{y_0=1/2}) = (2, 0)$; and a mirror TCP with $(\mathcal{V}^m_{\mathcal{S}}|_{y_0=0}, \mathcal{V}^m_{\mathcal{S}}|_{y_0=1/2}) = (0, 2)$. We illustrate the resulting markers in Figs. 3(c) and 3(d). We see that the marker for case (ii) [Fig. 3(c)] is localized around the center of the unit cell, while the marker for case (iii) [Fig. 3(d)] is localized halfway between unit cells.

To gain intuition about cases (ii) and (iii) we note that each mirror line having a nonvanishing invariant corresponds to a nontrivial 1D topological superconductor that must have Kramers' pairs of Majorana end modes on boundaries with normal vector $\pm\hat{x}$. In case (ii) such Majorana modes should arise along the edge at integer sites in the y direction, while in (iii) we expect them to be displaced to the midpoint between integers. This suggests that these phases could be distinguished by the location of Majorana modes along the edge.

To quantify this intuition, we examine the distribution of Wannier centers inside a unit cell $\mathcal{R}$ at the edge where a mirror line terminates. First, note that with a trivial strong index, the edge spectrum can always be detached from the bulk bands while preserving the DIII and mirror symmetries [see Fig. 3(b)]. By detaching the bands from the bulk we can define $\mathcal{P}_{\text{edge}}$ which is the projector into this spectrally detached Majorana band (DMB). Since $\mathcal{P}_{\text{edge}}$ includes positive and negative energies related by chiral symmetry, we can write it in terms of projectors into chiral subspaces

$$\mathcal{P}_{\text{edge}} = \sum_{\chi=\pm} \mathcal{P}^{\chi}_{\text{edge}}. \quad (17)$$

To characterize the position space structure of the edge modes we can consider the Wannier centers $\{e^{-2\pi i(R_y+\nu_{R_y j})/L_y}\}$ and Wannier functions $\{|\Psi^{\chi}_{R_y j}\rangle\}$ of the DMB that are obtained by diagonalizing the periodic projected position operator $\mathcal{W}^{\chi}_{\text{edge}} = \mathcal{P}^{\chi}_{\text{edge}} e^{-2\pi i\hat{Y}/L_y}\mathcal{P}^{\chi}_{\text{edge}}$ [45]; here, R_y labels unit cells along the edge, and j runs over the N_b states per unit cell included in the DMB. Using these Wannier centers, we can locally characterize the edge modes at $\mathcal{R}$ by the edge shift

$$\delta\mathcal{Y}^{\chi}_{\text{edge}}(\mathcal{R}) = \left(\sum_j \nu_{\mathcal{R}j}\right) \text{mod } 1, \quad (18)$$

where $\delta\mathcal{Y}^{+}_{\text{edge}}(\mathcal{R}) = \delta\mathcal{Y}^{-}_{\text{edge}}(\mathcal{R})$ from time-reversal symmetry. Furthermore, because of mirror symmetry $\delta\mathcal{Y}^{\chi}_{\text{edge}}(\mathcal{R}) = -\delta\mathcal{Y}^{\chi}_{\text{edge}}(\mathcal{R})$ mod 1. Thus, the edge shift must be quantized to either $\delta\mathcal{Y}^{\chi}_{\text{edge}}(\mathcal{R}) = 0$ or $\frac{1}{2}$.

Now, the value of $\delta\mathcal{Y}^{\chi}_{\text{edge}}(\mathcal{R})$ can be determined by the (parity of the) number of Wannier centers located at the symmetry centers in the unit cell at $\mathcal{R}$, and the mirror-related cell $\mathcal{R}'$. Hence, consider the pair of invariant points $S|_{y_0=1/2} = \{\mathcal{R} + \frac{1}{2}, \mathcal{R}' + \frac{1}{2}\}$. The Wannier states centered at these two symmetry centers are eigenstates of $\hat{m}_{\mathcal{S}}|_{y_0=1/2}$, whereas the remaining Wannier states come in mirror-related pairs. It follows that we can write the equality

$$\delta\mathcal{Y}^{\chi}_{\text{edge}}(\mathcal{R}) = \left[-\frac{i}{4}\sum_{R_y j}\left\langle\Psi^{\chi}_{R_y j}\right|(\hat{m}_{\mathcal{S}}|_{y_0=1/2})\left|\Psi^{\chi}_{R_y j}\right\rangle\right] \text{mod } 1, \quad (19)$$

which we derive in the Appendix. The sum can be replaced by a trace over the Hilbert space of the entire system to obtain $\delta\mathcal{Y}^{\chi}_{\text{edge}}(\mathcal{R}) = [\frac{1}{4}\Delta^m_{\mathcal{S}}|_{y_0=1/2}] \text{mod } 1$, where $\Delta^m_{\mathcal{S}} \equiv -\frac{i}{2}\text{Tr}[(\mathcal{P}_{\text{edge}}\hat{m}_{\mathcal{S}}\mathcal{P}_{\text{edge}})\chi]$. If we evaluate the edge invariant $\Delta^m_{\mathcal{S}}$ and use the connection between the bulk AIII winding invariant and the number of zero-energy boundary modes, then we find

$$\Delta^m_{\mathcal{S}} = \mathcal{V}^m_{\mathcal{S}}, \quad (20)$$

as we show in the Appendix. The edge shift is then determined by the bulk invariant

$$\delta\mathcal{Y}^{\chi}_{\text{edge}}(\mathcal{R}) = \left(\tfrac{1}{4}\mathcal{V}^m_{\mathcal{S}}\big|_{y_0=1/2}\right) \text{mod } 1. \quad (21)$$

We thus conclude that the two possible quantized edge shifts $(0, \frac{1}{2})$ are determined by the bulk and correspond to the two phases (ii) and (iii) we discussed earlier.

A remarkable by-product of this analysis reveals that the DMB is characterized by the integer topological invariant $\Delta^m_{\mathcal{S}}$ which must be equal to the bulk invariant $\mathcal{V}^m_{\mathcal{S}}$. Its topological marker is also exponentially localized at S along the edge and is robust to the presence of impurities at the edge. In Figs. 3(c) and 3(d) we illustrate the resulting topological markers of $\mathcal{V}^m_{\mathcal{S}}$ (labeled bulk marker) and $\Delta^m_{\mathcal{S}}$ (labeled edge marker) as well as representative Wannier functions $|\Psi^{\chi}_n|^2$ at the edge. In order

to numerically obtain the projector $\mathcal{P}_{\text{edge}}$ for a given edge, which is required for these calculations, we gapped out the boundary modes on the opposite edge (see Appendix). These results show that there is a clear correspondence between the bulk and edge topological markers that are centered at the mirror-invariant lines. Furthermore, the Wannier functions at the edge are centered at these mirror-invariant points as well, consistent with Eq. (21). Finally, the topological marker at the edge is localized, indicating that this edge invariant is indeed robust against the presence of impurities.

VI. CONCLUSIONS

In this work we have found that a large class of TCPs are characterized by a mesh of robustly quantized bulk and edge topological invariants that are constructed using projected symmetry operators. Our results constitute a starting point to further explore the real-space structure of other kinds of TCPs, for example, those on nonsymmorphic lattices. Furthermore, it suggests a pathway to study disordered systems with interactions by replacing single-particle projectors with Green's functions [46]. Finally, our findings point to the possibility of experimentally studying TCPs through local probes; for example, in ultracold atomic systems, where the single-particle projection operator can be extracted from time-of-flight measurements [47].

ACKNOWLEDGMENTS

We thank M. Hermele and S. Velury for useful conversations. I.M.S. gratefully acknowledges support by the Yale Prize Postdoctoral Fellowship. T.L.H. thanks the U.S. National Science Foundation (NSF) Grants No. EFMA-1627184 (EFRI) and No. DMR-1351895 (CAREER) and the support from the U.S. Office of Naval Research (ONR) Multidisciplinary University Research Initiative (MURI) under Grant No. N00014-20-1-2325.

APPENDIX: LOCALIZATION AND ROBUSTNESS OF TOPOLOGICAL MARKERS OF TCPs

1. General formulation of basis-independent topological invariants

a. Conventional momentum-space classification

Consider a translationally invariant d-dimensional system described by a Hamiltonian $\hat{H}$. Suppose the system is invariant under a spatial symmetry $G_{\mathcal{S}}$, where $\mathcal{S}$ denotes collectively the set of points that are left invariant by $G_{\mathcal{S}}$ in a system with periodic boundary conditions. If we denote by $\hat{g}_{\mathcal{S}}$ the Hilbert space representation of $G_{\mathcal{S}}$, then

$$[\hat{g}_{\mathcal{S}}, \hat{H}] = 0. \tag{A1}$$

Depending on the dimensionality of the system, when the spatial symmetry acts on a general position vector $\mathbf{r}$, it can leave invariant a subset of its components. We denote by $\mathbf{r}_I(\mathbf{r}_G)$ the components of $\mathbf{r}$ that are invariant (changed) by the operation $G_{\mathcal{S}}$. The number of components of $\mathbf{r}_I(\mathbf{r}_G)$ is $d_I(d_G)$ such that $d_I + d_G = d$.

We study the Bloch Hamiltonian $h(\mathbf{k})$ obtained by Fourier transforming *only* the spatial coordinates $\mathbf{r}_G$. Thus, $\mathbf{k}$ is a wave vector with d_G components. The momentum-space expression of $\hat{g}_{\mathcal{S}}$ is

$$\hat{g}_{\mathcal{S}} = \sum_{\mathbf{k}} \tilde{g}_{\mathcal{S}}(\mathbf{k}) \otimes |G_{\mathcal{S}}\mathbf{k}\rangle\langle\mathbf{k}|, \tag{A2}$$

so the action of the spatial symmetry on the Bloch Hamiltonian is then

$$\tilde{g}_{\mathcal{S}}(\mathbf{k}) h(\mathbf{k}) \tilde{g}_{\mathcal{S}}^{-1}(\mathbf{k}) = h(G_{\mathcal{S}}\mathbf{k}). \tag{A3}$$

At the momenta $\mathbf{k}^{\text{inv}}$ that are invariant under $G_{\mathcal{S}}$, we have

$$[\tilde{g}_{\mathcal{S}}(\mathbf{k}^{\text{inv}}), h(\mathbf{k}^{\text{inv}})] = 0. \tag{A4}$$

Thus, the occupied states $\{|u^n_{j\mathbf{k}^{\text{inv}}}\rangle\}$ can be classified according to the eigenvalues $\{e^{i\phi_j(\mathbf{k}^{\text{inv}})}\}$ of $\tilde{g}_{\mathcal{S}}(\mathbf{k}^{\text{inv}})$. Let us denote the projector into the occupied eigenstates of a given subspace by $\mathcal{P}_{j\mathbf{k}^{\text{inv}}} = \sum_{n\in\text{occ}} |u^n_{j\mathbf{k}^{\text{inv}}}\rangle\langle u^n_{j\mathbf{k}^{\text{inv}}}|$. The conventional classification of a large class of TCPs is based on determining the topology encoded by $\mathcal{P}_{j\mathbf{k}^{\text{inv}}}$.

The set of topological invariants $\{\tau_j(\mathbf{k}^{\text{inv}})\}$ that characterize the invariant subspaces depend on their effective dimensionality d_s and the other symmetries of the system. Examples of possible invariants that could be relevant include occupation numbers (e.g., [9]), winding numbers (e.g., [12]), and Chern numbers (e.g., [3]). Such topological invariants $\{\tau_j(\mathbf{k}^{\text{inv}})\}$ can generally be written as the average over occupied states of an operator $\mathcal{F}$ that is a function of $\mathcal{P}_{j\mathbf{k}^{\text{inv}}}$:

$$\tau_j(\mathbf{k}_{\text{inv}}) = \text{Tr}_\circ\big[\mathcal{F}\big(\mathcal{P}_{j\mathbf{k}_{\text{inv}}}\big)\big], \tag{A5}$$

where $\text{Tr}_\circ$ refers to the trace over the nonspatial degrees of freedom as well as the d_I spatial degrees of freedom that do not get transformed by $G_{\mathcal{S}}$. For a broad range of TCPs, the function $\mathcal{F}$ is written as a sum of products of projection operators and position operators that are components of $\mathbf{r}_I$, such that it projects the trace into a sum over occupied states. Examples of the form of $\mathcal{F}$ are

$$\mathcal{F}(\mathcal{P}) \propto \begin{cases} \mathcal{P} & \text{(e.g., 0D occupation number [9] for 1D TCP)}, \\ \mathcal{P}[\hat{X}, \mathcal{P}] & \text{(e.g., 1D winding number [44] for 2D TCP)}, \\ \mathcal{P}[[\hat{X}, \mathcal{P}], [\hat{Y}, \mathcal{P}]] & \text{(e.g., 2D Chern number [48] for 3D TCP)}, \end{cases} \tag{A6}$$

where $\hat{X}, \hat{Y}$ are the x, y components of the position operator. These commutators are the basis-independent generalizations of momentum-space derivatives that naturally arise in the calculations of Berry connections.

b. Basis-independent topological invariants of TCPs

We now set out to obtain topological invariants with localized topological markers using the momentum-space invariants $\{\tau_j(\mathbf{k}^{\text{inv}})\}$. Let us now define the

quantities

$$T_{\mathcal{S}}^{g} \equiv \sum_{j,\mathbf{k}^{\mathrm{inv}}} e^{i\phi_j(\mathbf{k}^{\mathrm{inv}})}\tau_j(\mathbf{k}^{\mathrm{inv}}). \tag{A7}$$

Since the $\{T_{\mathcal{S}}^{g}\}$ are linear combinations of the momentum-space topological invariants, they are themselves topological invariants of the TCP. We will now show that these topological invariants have topological markers that are exponentially localized and are robust to the presence of impurities in the system. This will be done by expressing them in terms of the projector in the full ground state given by

$$\mathcal{P}_G = \sum_{j\mathbf{k}} \mathcal{P}_{\mathbf{k}j}. \tag{A8}$$

We can rewrite them in a basis-independent form

$$T_{\mathcal{S}}^{g} = \sum_{j,\mathbf{k}^{\mathrm{inv}}} e^{i\phi_j(\mathbf{k}^{\mathrm{inv}})}\tau_j(\mathbf{k}^{\mathrm{inv}}) \tag{A9}$$

$$= \sum_{j,\mathbf{k}^{\mathrm{inv}}} \mathrm{Tr}_{\circ}[e^{i\phi_j(\mathbf{k}^{\mathrm{inv}})}\mathcal{F}(\mathcal{P}_{j,\mathbf{k}^{\mathrm{inv}}})] \tag{A10}$$

$$= \sum_{j,\mathbf{k}^{\mathrm{inv}}} \mathrm{Tr}_{\circ}\left[e^{i\phi_j(\mathbf{k}^{\mathrm{inv}})}\mathcal{P}_{j\mathbf{k}_{\mathrm{inv}}}\mathcal{F}(\mathcal{P}_{j,\mathbf{k}^{\mathrm{inv}}})\right] \tag{A11}$$

$$= \sum_{j,\mathbf{k}^{\mathrm{inv}}} \mathrm{Tr}_{\circ}[\mathcal{P}_{j\mathbf{k}^{\mathrm{inv}}}e^{i\phi_j(\mathbf{k}^{\mathrm{inv}})}\mathcal{P}_{j\mathbf{k}^{\mathrm{inv}}}\mathcal{F}(\mathcal{P}_{j,\mathbf{k}^{\mathrm{inv}}})]. \tag{A12}$$

Now, since $\hat{\mathbf{r}}_I$ and $\mathcal{P}_{j\mathbf{k}^{\mathrm{inv}}}$ commute with $\widetilde{g}_{\mathcal{S}}(\mathbf{k}^{\mathrm{inv}})$, then $[\widetilde{g}_{\mathcal{S}}(\mathbf{k}^{\mathrm{inv}}), \mathcal{F}(\mathcal{P}_{j\mathbf{k}^{\mathrm{inv}}})] = 0$. This implies that $\mathcal{F}(\mathcal{P}_{j\mathbf{k}^{\mathrm{inv}}})$ is block diagonal in the basis of $\widetilde{g}_{\mathcal{S}}(\mathbf{k}^{\mathrm{inv}})$, and we can thus write $\sum_j \mathcal{F}(\mathcal{P}_{j\mathbf{k}^{\mathrm{inv}}}) = \mathcal{F}(\sum_j \mathcal{P}_{j\mathbf{k}^{\mathrm{inv}}})$. Furthermore, by assumption, the terms that make up $\mathcal{F}(\mathcal{P}_G)$ are invariant under translations along the components of $\hat{\mathbf{r}}_G$. This means that $\mathcal{F}$ is block diagonal with respect to $\mathbf{k}$. As a consequence

$$\sum_{\mathbf{k}} \mathcal{F}(\mathcal{P}_{\mathbf{k}}) \otimes |\mathbf{k}\rangle\langle\mathbf{k}| = \mathcal{F}\left(\sum_{\mathbf{k}} \mathcal{P}_{\mathbf{k}} \otimes |\mathbf{k}\rangle\langle\mathbf{k}|\right) \tag{A13}$$

$$= \mathcal{F}(\mathcal{P}_G). \tag{A14}$$

Using these properties of $\mathcal{F}$, we then obtain

$$T_{\mathcal{S}}^{g} = \sum_{\mathbf{k}^{\mathrm{inv}}} \mathrm{Tr}_{\circ}\left[\left(\sum_{j_1} \mathcal{P}_{j_1\mathbf{k}^{\mathrm{inv}}}\right)\widetilde{g}_{\mathcal{S}}(\mathbf{k}^{\mathrm{inv}})\left(\sum_{j_2} \mathcal{P}_{j_2\mathbf{k}^{\mathrm{inv}}}\right)\mathcal{F}\left(\sum_{j_3} \mathcal{P}_{j_3\mathbf{k}^{\mathrm{inv}}}\right)\right] \tag{A15}$$

$$= \sum_{\mathbf{k}^{\mathrm{inv}}} \mathrm{Tr}_{\circ}[(\mathcal{P}_{\mathbf{k}^{\mathrm{inv}}})\widetilde{g}_{\mathcal{S}}(\mathbf{k}^{\mathrm{inv}})(\mathcal{P}_{\mathbf{k}^{\mathrm{inv}}})(\mathcal{F}(\mathcal{P}_{\mathbf{k}^{\mathrm{inv}}}))] \tag{A16}$$

$$= \sum_{\mathbf{k}^{\mathrm{inv}}} \langle\mathbf{k}^{\mathrm{inv}}|\mathrm{Tr}_{\circ}[(\mathcal{P}_{\mathbf{k}^{\mathrm{inv}}} \otimes |\mathbf{k}^{\mathrm{inv}}\rangle\langle\mathbf{k}^{\mathrm{inv}}|)(\tilde{g}_{\mathcal{S}}(\mathbf{k}^{\mathrm{inv}}) \otimes |\mathbf{k}^{\mathrm{inv}}\rangle\langle\mathbf{k}^{\mathrm{inv}}|).$$
$$\times (\mathcal{P}_{\mathbf{k}^{\mathrm{inv}}} \otimes |\mathbf{k}^{\mathrm{inv}}\rangle\langle\mathbf{k}^{\mathrm{inv}}|)(\mathcal{F}(\mathcal{P}_{\mathbf{k}^{\mathrm{inv}}}) \otimes |\mathbf{k}^{\mathrm{inv}}\rangle\langle\mathbf{k}^{\mathrm{inv}}|)]|\mathbf{k}^{\mathrm{inv}}\rangle \tag{A17}$$

$$= \sum_{\mathbf{k}^{\mathrm{inv}}} \langle\mathbf{k}^{\mathrm{inv}}|\mathrm{Tr}_{\circ}\left[\left(\sum_{\mathbf{q}_1} \mathcal{P}_{\mathbf{q}_1} \otimes |\mathbf{q}_1\rangle\langle\mathbf{q}_1|\right)\left(\sum_{\mathbf{q}_2} \tilde{g}_{\mathcal{S}}(\mathbf{q}_2) \otimes |G_{\mathcal{S}}\mathbf{q}_2\rangle\langle\mathbf{q}_2|\right)\right.$$
$$\left.\times \left(\sum_{\mathbf{q}_3} \mathcal{P}_{\mathbf{q}_3} \otimes |\mathbf{q}_3\rangle\langle\mathbf{q}_3|\right)\left(\sum_{\mathbf{q}_4} \mathcal{F}(\mathcal{P}_{\mathbf{q}_4}) \otimes |\mathbf{q}_4\rangle\langle\mathbf{q}_4|\right)\right]|\mathbf{k}^{\mathrm{inv}}\rangle$$

$$= \sum_{\mathbf{k}} \langle\mathbf{k}|\mathrm{Tr}_{\circ}\left[\left(\sum_{\mathbf{q}_1} \mathcal{P}_{\mathbf{q}_1} \otimes |\mathbf{q}_1\rangle\langle\mathbf{q}_1|\right)\left(\sum_{\mathbf{q}_2} \tilde{g}_{\mathcal{S}}(\mathbf{q}_2) \otimes |G_{\mathcal{S}}\mathbf{q}_2\rangle\langle\mathbf{q}_2|\right)\right.$$
$$\left.\times \left(\sum_{\mathbf{q}_3} \mathcal{P}_{\mathbf{q}_3} \otimes |\mathbf{q}_3\rangle\langle\mathbf{q}_3|\right)\mathcal{F}\left(\sum_{\mathbf{q}_4} \mathcal{P}_{\mathbf{q}_4} \otimes |\mathbf{q}_4\rangle\langle\mathbf{q}_4|\right)\right]|\mathbf{k}\rangle \tag{A18}$$

$$= \sum_{\mathbf{k}} \langle\mathbf{k}|\mathrm{Tr}_{\circ}[\mathcal{P}_G\hat{g}_{\mathcal{S}}\mathcal{P}_G\mathcal{F}(\mathcal{P}_G)]|\mathbf{k}\rangle \tag{A19}$$

$$= \mathrm{Tr}[\overline{g}_{\mathcal{S}}\mathcal{F}(\mathcal{P}_{\mathrm{G}})], \tag{A20}$$

which is the basis-independent expression quoted in the main text for these topological invariants.

c. Localized topological markers

We now show that the presence of the projected symmetry operator $\overline{g}_{\mathcal{S}}$ in our expression for $T_{\mathcal{S}}^{g}$ implies that the topological markers are spatially localized. Consider a position $\mathbf{r}_G$ far away from the fixed points $\mathcal{S}$ (a condition we denote by $|\mathcal{S} - \mathbf{r}_G| \gg \zeta$), which implies that $|G_{\mathcal{S}}\mathbf{r}_G - \mathbf{r}_G| \gg \zeta$. We know that for gapped systems, the projection operator has the long-distance behavior

$$|\langle\mathbf{r}_{G_1}, \alpha|\mathcal{P}_G|\mathbf{r}_{G_2}, \beta\rangle| < O(e^{-|\mathbf{r}_{G_1} - \mathbf{r}_{G_2}|/\zeta}), \tag{A21}$$

when $\zeta \ll |\mathbf{r}_{G_1} - \mathbf{r}_{G_2}|$ where α, β denote all internal and remaining spatial degrees of freedom. Furthermore, since $\mathcal{F}$ is

only dependent on $\mathcal{P}_G$ and the components of $\hat{\mathbf{r}}_I$, then

$$|\langle \mathbf{r}_{G_1}, \alpha|\mathcal{F}(\mathcal{P}_G)|\mathbf{r}_{G_2}, \beta\rangle| < O(e^{-|\mathbf{r}_{G_1}-\mathbf{r}_{G_2}|/\zeta}) \tag{A22}$$

when $\zeta \ll |\mathbf{r}_{G_1} - \mathbf{r}_{G_2}|$. Using this, we can then write the topological marker $\mathcal{T}^g_{\mathcal{S}}(\mathbf{r}_G) = \langle \mathbf{r}_G|\mathrm{Tr}_\circ[\bar{g}_{\mathcal{S}}\mathcal{F}(\mathcal{P}_G)]|\mathbf{r}_G\rangle$ as

$$\begin{aligned}
\mathcal{T}^g_{\mathcal{S}}(\mathbf{r}_G) &= \mathrm{Tr}_\circ[\langle \mathbf{r}'_G|\hat{g}_{\mathcal{S}}\mathcal{P}_G\mathcal{F}(\mathcal{P}_\mathrm{G})|\mathbf{r}_G\rangle] && \text{(A23)}\\
&= \sum_{\mathbf{r}_{G1}\mathbf{r}_{G2}} \mathrm{Tr}_\circ[\langle \mathbf{r}_G|\hat{g}_{\mathcal{S}}|\mathbf{r}_{G1}\rangle\langle \mathbf{r}_{G1}|\mathcal{P}_G|\mathbf{r}_{G2}\rangle\langle \mathbf{r}_{G2}|\mathcal{F}(\mathcal{P}_\mathrm{G})|\mathbf{r}_G\rangle] && \text{(A24)}\\
&= \sum_{\mathbf{r}_{G1}\mathbf{r}_{G2}} \mathrm{Tr}_\circ[\delta_{\mathbf{r}_G, G_{\mathcal{S}}\mathbf{r}_{G1}}\langle \mathbf{r}_{G1}|\mathcal{P}_G|\mathbf{r}_{G2}\rangle\langle \mathbf{r}_{G2}|\mathcal{F}(\mathcal{P}_\mathrm{G})|\mathbf{r}_G\rangle] && \text{(A25)}\\
&= \sum_{\mathbf{r}_{G2}} \mathrm{Tr}_\circ\big[\big\langle G^{-1}_{\mathcal{S}}\mathbf{r}_G\big|\mathcal{P}_G|\mathbf{r}_{G2}\rangle\langle \mathbf{r}_{G2}|\mathcal{F}(\mathcal{P}_\mathrm{G})|\mathbf{r}_G\rangle\big] && \text{(A26)}\\
&= \sum_{|\mathbf{r}_{G2}-\mathbf{r}_G|<\zeta} \mathrm{Tr}_\circ\big[\big\langle G^{-1}_{\mathcal{S}}\mathbf{r}_G\big|\mathcal{P}_G|\mathbf{r}_{G2}\rangle\langle \mathbf{r}_{G2}|\mathcal{F}(\mathcal{P}_\mathrm{G})|\mathbf{r}_G\rangle\big] + \sum_{|\mathbf{r}_{G2}-G^{-1}_{\mathcal{S}}\mathbf{r}_G|<\zeta} \mathrm{Tr}_\circ\big[\big\langle G^{-1}_{\mathcal{S}}\mathbf{r}_G\big|\mathcal{P}_G|\mathbf{r}_{G2}\rangle\langle \mathbf{r}_{G2}|\mathcal{F}(\mathcal{P}_\mathrm{G})|\mathbf{r}_G\rangle\big] && \text{(A27)}\\
&\quad + \sum_{\substack{|\mathbf{r}_{G2}-G^{-1}_{\mathcal{S}}\mathbf{r}_G|>\zeta\\ |\mathbf{r}_{G2}-\mathbf{r}_G|>\zeta}} \mathrm{Tr}_\circ\big[\big\langle G^{-1}_{\mathcal{S}}\mathbf{r}_G\big|\mathcal{P}_G|\mathbf{r}_{G2}\rangle\langle \mathbf{r}_{G2}|\mathcal{F}(\mathcal{P}_\mathrm{G})|\mathbf{r}_G\rangle\big]. && \text{(A28)}
\end{aligned}$$

Now, we have that

$$A_1 = \left|\sum_{|\mathbf{r}_{G2}-\mathbf{r}_G|<\zeta} \mathrm{Tr}\big[\big\langle G^{-1}_{\mathcal{S}}\mathbf{r}_G\big|\mathcal{P}_G|\mathbf{r}_{G2}\rangle\langle \mathbf{r}_{G2}|\mathcal{F}(\mathcal{P}_\mathrm{G})|\mathbf{r}_G\rangle\big]\right| < O(e^{-|G^{-1}_{\mathcal{S}}\mathbf{r}_G-\mathbf{r}_G|/\zeta}), \tag{A29}$$

$$A_2 = \left|\sum_{|\mathbf{r}_{G2}-G^{-1}_{\mathcal{S}}\mathbf{r}_G|<\zeta} \mathrm{Tr}\big[\big\langle G^{-1}_{\mathcal{S}}\mathbf{r}_G\big|\mathcal{P}_G|\mathbf{r}_{G2}\rangle\langle \mathbf{r}_{G2}|\mathcal{F}(\mathcal{P}_\mathrm{G})|\mathbf{r}_G\rangle\big]\right| < O(e^{-|G^{-1}_{\mathcal{S}}\mathbf{r}_G-\mathbf{r}_G|/\zeta}), \tag{A30}$$

$$A_3 = \left|\sum_{\substack{|\mathbf{r}_{G2}-G^{-1}_{\mathcal{S}}\mathbf{r}_G|>\zeta\\ |\mathbf{r}_{G2}-\mathbf{r}_G|>\zeta}} \mathrm{Tr}\big[\big\langle G^{-1}_{\mathcal{S}}\mathbf{r}_G\big|\mathcal{P}_G|\mathbf{r}_{G2}\rangle\langle \mathbf{r}_{G2}|\mathcal{F}(\mathcal{P}_\mathrm{G})|\mathbf{r}_G\rangle\big]\right| \ll A_{1,2}. \tag{A31}$$

We thus conclude that

$$\big|\mathcal{T}^g_{\mathcal{S}}(\mathbf{r}_G)\big| < O(e^{-|G_{\mathcal{S}}\mathbf{r}_G-\mathbf{r}_G|/\zeta}) \quad \text{when } \zeta \ll |G_{\mathcal{S}}\mathbf{r}_G - \mathbf{r}_G|, \tag{A32}$$

which implies that the topological marker is concentrated around the fixed points of the spatial symmetry.

d. Robustness to impurities placed far from fixed points

We now show that although the conventional momentum-space invariants cannot be used in the presence of impurities, the invariants $T^g_{\mathcal{S}}$ can remain robustly quantized. Suppose we add an impurity $V_{\mathrm{imp}}(\mathbf{r}) = V_0\delta_{\mathbf{r},\mathbf{R}_0}$ at a position $\mathbf{R}_0$. The projection operator of the new ground state can be written as $\mathcal{P}'_G = \mathcal{P}_G + \delta\mathcal{P}_G$. Since the system is gapped, $\delta\mathcal{P}_G$ only has support in an exponentially small neighborhood of size ζ centered at the impurity:

$$|\langle \mathbf{r}_G, \alpha|\delta\mathcal{P}_G|\mathbf{R}_0, \beta\rangle| < O(e^{-(|\mathbf{r}_G-\mathbf{R}_0|)/\zeta}). \tag{A33}$$

Let us now define a function $\Gamma(\mathcal{P}'_G)$ by

$$\delta\Gamma(\mathcal{P}'_G) \equiv \mathcal{P}'_G\mathcal{F}(\mathcal{P}'_G) - \mathcal{P}_G\mathcal{F}(\mathcal{P}_G). \tag{A34}$$

The function $\Gamma(\mathcal{P}'_G)$ must vanish when $\delta\mathcal{P}_G = 0$, so it must be a sum of terms all of which possess at least one factor of $\delta\mathcal{P}_G$. It follows that

$$|\langle \mathbf{r}_G, \alpha|\Gamma(\mathcal{P}'_G)|\mathbf{R}_0, \beta\rangle| < O(e^{-|\mathbf{r}_G-\mathbf{R}_0|/\zeta}) \tag{A35}$$

for $|\mathbf{r}_G - \mathbf{R}_0| \gg \zeta$. For an impurity placed far away from the points in $\mathcal{S}$, the topological invariant is modified as

$$\begin{aligned}
T^{g'}_{\mathcal{S}}(\mathbf{R}_0) - T^g_{\mathcal{S}} &= \mathrm{Tr}[\hat{g}_{\mathcal{S}}\Gamma(\mathcal{P}'_G)]\\
&= \sum_{\mathbf{r}_G\mathbf{r}_{G1}} \mathrm{Tr}_\circ[\langle \mathbf{r}_G|\hat{g}_{\mathcal{S}}|\mathbf{r}_{G1}\rangle\langle \mathbf{r}_{G1}|\Gamma(\mathcal{P}'_G)|\mathbf{r}_G\rangle]\\
&= \sum_{\mathbf{r}_G\mathbf{r}_{G1}} \mathrm{Tr}_\circ\big[\delta_{\mathbf{r}_G, G_{\mathcal{S}}\mathbf{r}_{G1}}\langle \mathbf{r}_{G1}|\Gamma(\mathcal{P}'_G)|\mathbf{r}_G\rangle\big]\\
&= \sum_{\mathbf{r}_G} \mathrm{Tr}_\circ\big[\big\langle G^{-1}_{\mathcal{S}}\mathbf{r}_G\big|\Gamma(\mathcal{P}'_G)|\mathbf{r}_G\rangle\big]\\
&= \sum_{|G^{-1}_{\mathcal{S}}\mathbf{r}_G-\mathbf{R}_0|<\zeta} \mathrm{Tr}_\circ\big[\big\langle G^{-1}_{\mathcal{S}}\mathbf{r}_G\big|\Gamma(\mathcal{P}'_G)|\mathbf{r}_G\rangle\big]
\end{aligned}$$

$$+\sum_{|\mathbf{r}_G-\mathbf{R}_0|<\zeta}\mathrm{Tr}_\circ\big[\langle G_{\mathcal{S}}^{-1}\mathbf{r}_G|\Gamma(\mathcal{P}'_G)|\mathbf{r}_G\rangle\big]$$
$$+\sum_{\substack{|G_{\mathcal{S}}^{-1}\mathbf{r}_G-\mathbf{R}_0|>\zeta\\ |\mathbf{r}_G-\mathbf{R}_0|>\zeta}}\mathrm{Tr}_\circ\big[\langle G_{\mathcal{S}}^{-1}\mathbf{r}_G|\Gamma(\mathcal{P}'_G)|\mathbf{r}_G\rangle\big]. \tag{A36}$$

Now, we have that

$$B_1=\left|\sum_{|G_{\mathcal{S}}^{-1}\mathbf{r}_G-\mathbf{R}_0|<\zeta}\mathrm{Tr}_\circ\big[\langle G_{\mathcal{S}}^{-1}\mathbf{r}_G|\Gamma(\mathcal{P}'_G)|\mathbf{r}_G\rangle\big]\right|$$
$$<O(e^{-|\mathbf{R}_0-G_{\mathcal{S}}\mathbf{R}_0|/\zeta}), \tag{A37}$$

$$B_2=\left|\sum_{|\mathbf{r}_G-\mathbf{R}_0|<\zeta}\mathrm{Tr}_\circ\big[\langle G_{\mathcal{S}}^{-1}\mathbf{r}_G|\Gamma(\mathcal{P}'_G)|\mathbf{r}_G\rangle\big]\right|$$
$$<O(e^{-|G_{\mathcal{S}}^{-1}\mathbf{R}_0-\mathbf{R}_0|/\zeta}), \tag{A38}$$

$$B_3=\left|\sum_{\substack{|G_{\mathcal{S}}^{-1}\mathbf{r}_G-\mathbf{R}_0|>\zeta\\ |\mathbf{r}_G-\mathbf{R}_0|>\zeta}}\mathrm{Tr}_\circ\big[\langle G_{\mathcal{S}}^{-1}\mathbf{r}_G|\Gamma(\mathcal{P}'_G)|\mathbf{r}_G\rangle\big]\right|$$
$$\ll B_{1,2}. \tag{A39}$$

We thus conclude that

$$\big|T_{\mathcal{S}}^{g'}(\mathbf{R}_0)-T_{\mathcal{S}}^{g}\big|<O(e^{-|G_{\mathcal{S}}\mathbf{R}_0-\mathbf{R}_0|/\zeta}), \tag{A40}$$

which implies that impurities in the system will not affect the quantization of the invariants $T_{\mathcal{S}}^{g}$ as long their distance to $\mathcal{S}$ is many times bigger than a correlation length ζ.

2. Inversion-symmetric topological insulators in one dimension

a. Conventional classification

Consider topological insulators in one-dimensional protected by inversion symmetry. With periodic boundary conditions, an inversion-symmetry operation $P_{\mathcal{S}}$ leaves invariant two positions $\mathcal{S}=\{R+r_0, R+1+L_x/2+r_0\}$ on the lattice with $R\leqslant L_x/2$. The number r_0 is a fixed position within the unit cell that can take the values 0 or $\frac{1}{2}$, where we set the unit-cell length to be $a=1$. Consider the momentum-space expansion of the inversion operator

$$\hat{p}_{\mathcal{S}}=\sum_{k_x}\widetilde{p}_{\mathcal{S}}(k_x)\otimes|P_{\mathcal{S}}k_x\rangle\langle k_x|. \tag{A41}$$

The conventional momentum-space classification is based on counting the number of occupied states $n_{\mathcal{S}}^{\pm}(k_x^{\mathrm{inv}})$ with eigenvalues of the operator $\widetilde{p}_{\mathcal{S}}(k_x)$ at the invariant momenta $k_x^{\mathrm{inv}}=0,\pi$. The invariant is given by [33]

$$\Delta_{\mathcal{S}}^{p}=\sum_{k_x=0,\pi}[n_{\mathcal{S}}^{(+)}(k_x)-n_{\mathcal{S}}^{(-)}(k_x)],$$

which is an integer invariant.

b. Basis-independent classification

We now discuss the topological invariants $T_{\mathcal{S}}^{p}$ for this TCP. The topological invariants at the invariant momenta are

$$\tau_{\pm}\big(k_x^{\mathrm{inv}}\big)=n_{\mathcal{S}}^{\pm}\big(k_x^{\mathrm{inv}}\big)=\mathrm{Tr}_\circ\big[\mathcal{P}_{\pm,k_x^{\mathrm{inv}}}\big]. \tag{A42}$$

It is clear then that, in this case, $\mathcal{F}(\mathcal{P}_{\pm,k_x^{\mathrm{inv}}})=\mathcal{P}_{\pm,k_x^{\mathrm{inv}}}$. By using these invariants in Eq. (A20), we find

$$T_{\mathcal{S}}^{p}=\sum_{k_x=0,\pi}[(+1)n_{\mathcal{S}}^{(+)}(k_x)+(-1)n_{\mathcal{S}}^{(-)}(k_x)]$$
$$=\mathrm{Tr}\big[\overline{p}_{\mathcal{S}}\cdot\mathcal{P}_{\pm,k_x^{\mathrm{inv}}}\big]=\mathrm{Tr}[\overline{p}_{\mathcal{S}}].$$

In this particular example, the linear combination $T_{\mathcal{S}}^{p}$ of momentum-space topological invariants is precisely the topological invariant $\Delta_{\mathcal{S}}^{p}$ that was proposed for these TCPs [33]. The topological marker for this invariant satisfies

$$\big|\mathcal{T}_{\mathcal{S}}^{p}(x)\big|<O(e^{-2|x-\mathcal{S}|/\zeta}), \tag{A43}$$

when $\zeta\ll|x-\mathcal{S}|$ and an impurity placed at $x=X_0$ will change an invariant centered at $\mathcal{S}$ by an exponentially small amount

$$\big|T_{\mathcal{S}}^{p'}(X_0)-T_{\mathcal{S}}^{p}\big|<O(e^{-2|X_0-\mathcal{S}|/\zeta}), \tag{A44}$$

when $\zeta\ll|X_0-\mathcal{S}|$ where the notation $|X_0-\mathcal{S}|$ means the shortest distance to any of the invariant points in the set $\mathcal{S}$.

3. Rotationally symmetric topological superconductors in two dimensions

a. Conventional classification

Consider topological superconductors in the absence of time-reversal symmetry and protected by rotational symmetries. With periodic boundary conditions, a given n-fold rotation operation $C_{\mathcal{S}}^{(n)}$ leaves invariant a set $\mathcal{S}=\{\mathbf{R}_i+\mathbf{r}_0\}$ of positions on the lattice. In particular, we will consider models that satisfy $[\hat{c}_{\mathcal{S}}^{(n=2,4)},\hat{H}]=0$, where $\hat{c}_{\mathcal{S}}^{(n)}$ is the Hilbert space representation of $C_{\mathcal{S}}^{(n)}$. By denoting the primitive vectors as $2\mathbf{a}_1$ and $2\mathbf{a}_2$, then fourfold rotations allow the positions $\mathbf{r}_0\in\{\mathbf{0},\mathbf{a}_1+\mathbf{a}_2\}$, whereas twofold rotations allow $\mathbf{r}_0\in\{\mathbf{0},\mathbf{a}_1,\mathbf{a}_2,\mathbf{a}_1+\mathbf{a}_2\}$. Consider the momentum-space expansion of the rotation operators

$$\hat{c}_{\mathcal{S}}^{(n)}=\sum_{\mathbf{k}}\widetilde{c}_{\mathcal{S}}^{(n)}(\mathbf{k})\otimes\big|C_{\mathcal{S}}^{(n)}\mathbf{k}\big\rangle\langle\mathbf{k}|. \tag{A45}$$

The conventional momentum-space classification is based on counting eigenvalues of the specific operator $\widetilde{c}_{\mathcal{S}}^{(n)}(\mathbf{k})|_{\mathbf{r}_0=\mathbf{0}}$. For a given invariant momentum $\mathbf{\Pi}^{(n)}(=\Gamma,X,M_i)$, the possible eigenvalues of $\widetilde{c}_{\mathcal{S}}^{(n)}(\mathbf{k})|_{\mathbf{r}_0=\mathbf{0}}$ are $\Pi_p^{(n)}=e^{i\pi(2p-1)/n}$, for $p=1,2,\ldots,n$. Let us denote by $\#\Pi_p^{(n)}$ the number of occupied states with eigenvalue $\Pi_p^{(n)}$ at the momentum $\mathbf{\Pi}^{(n)}$. The topological invariants are then obtained by defining a relative occupation number

$$\big[\Pi_p^{(n)}\big]=\#\Pi_p^{(n)}-\#\Gamma_p^{(n)}. \tag{A46}$$

In particular, as we mentioned in the main text, the topological invariants for systems that are symmetric under fourfold rotations are ($[X]$, $[M_1]$, $[M_2]$).

b. Basis-independent classification

We now proceed to adapt Eq. (A20) to these TCPs. We define the topological invariants of the invariant subspaces as the occupation numbers $n_{\mathcal{S}}^{(n,p)}(\mathbf{\Pi}^{(n)})$ of the eigenvalues of the operator $\widetilde{c}_{\mathcal{S}}^{(n)}(\mathbf{k})$:

$$\tau_{np}(\mathbf{\Pi}^{(n)}) = n_{\mathcal{S}}^{(n,p)}(\mathbf{\Pi}^{(n)}) = \mathrm{Tr}_{\circ}[\mathcal{P}_{j\mathbf{k}^{\mathrm{inv}}}], \tag{A47}$$

where we again have used $\mathcal{F}(\mathcal{P}_{j\mathbf{k}^{\mathrm{inv}}}) = \mathcal{P}_{j\mathbf{k}^{\mathrm{inv}}}$. From Eq. (A20), we know that this implies that

$$T_{\mathcal{S}}^{c(n)} = \mathrm{Tr}\big[\bar{c}_{\mathcal{S}}^{(n)}\mathcal{F}(\mathcal{P}_G)\big] = \mathrm{Tr}\big[\bar{c}_{\mathcal{S}}^{(n)}\big]. \tag{A48}$$

In contrast with the inversion-symmetric case, the conventional momentum-space topological invariants are not exactly the invariants $T_{\mathcal{S}}^{c(n)}$. We can, nevertheless, find a relation between both. The rotation operator at an invariant momentum for a given set of fixed points $\mathcal{S}$ can be written in the form

$$\widetilde{c}_{\mathcal{S}}^{(n)}(\mathbf{k}) = \big[\widetilde{c}_{\mathcal{S}}^{(n)}(\mathbf{k})\big|_{\mathbf{r}_0=\mathbf{0}}\big]e^{i(C_{\mathcal{S}}^{(n)}\mathbf{\Pi}^{(n)}-\mathbf{\Pi}^{(n)})\cdot\mathbf{r}_0}, \tag{A49}$$

which implies that their eigenvalues are

$$e^{i\phi_{np}(\mathbf{\Pi}^{(n)})} = e^{i(\pi(2p-1)/n+(C_{\mathcal{S}}^{(n)}\mathbf{\Pi}^{(n)}-\mathbf{\Pi}^{(n)})\cdot\mathbf{r}_0)}. \tag{A50}$$

Since the $\mathbf{\Pi}^{(n)}$ are invariant momenta under rotations by definition, $(C_{\mathcal{S}}^{(n)}\mathbf{\Pi}^{(n)} - \mathbf{\Pi}^{(n)})\cdot\mathbf{r}_0 = \sum_i m_i\mathbf{b}_i$ where the $m_{1,2}$ are integers and the $\mathbf{b}_{1,2}$ are primitive vectors in reciprocal space that satisfy $\mathbf{b}_i\cdot(2\mathbf{a}_j) = 2\pi\delta_{ij}$. With these definitions, the traces of the projected rotation operators for $n = 4$ can be written as

$$T_{\mathcal{S}}^{c(4)} = \sum_{p=1}^{4}\left(e^{i\phi_{4p}(\mathbf{\Gamma})}n_{\mathcal{S}}^{(4,p)}(\mathbf{\Gamma}) + e^{i\phi_{4p}(\mathbf{M})}n_{\mathcal{S}}^{(4,p)}(\mathbf{M})\right) \tag{A51}$$

$$= \sum_{p=1}^{4}(e^{i\pi(2p-1)/4}\#\Gamma_p + e^{i\pi(2p-1)/4-i\mathbf{b}_1\cdot\mathbf{r}_0}\#M_p) \tag{A52}$$

$$= \sum_{p=1}^{4}e^{i\pi(2p-1)/4}[(1+e^{-i\mathbf{b}_1\cdot\mathbf{r}_0})\#\Gamma_p + e^{-i\mathbf{b}_1\cdot\mathbf{r}_0}[M_p]]$$

$$= \left\{\left(1+e^{-i\mathbf{b}_1\cdot\mathbf{r}_0}\right)\left(\sum_p e^{i\pi(2p-1)/4}\#\Gamma_p\right) + i\sqrt{2}e^{-i\mathbf{b}_1\cdot\mathbf{r}_0}([M_1]+[M_2])\right\}, \tag{A53}$$

where we have used that $[M_1] = -[M_4]$ and $[M_2] = -[M_3]$ due to particle-hole symmetry. For the $n = 2$ case, the topological invariants are

$$\begin{aligned}T_{\mathcal{S}}^{c(2)} &= \sum_p\left(e^{i\phi_{2p}(\mathbf{\Gamma})}n_{\mathcal{S}}^{(2,p)}(\mathbf{\Gamma}) + e^{i\phi_{2p}(\mathbf{M})}n_{\mathcal{S}}^{(2,p)}(\mathbf{M})\right) = i((\#\Gamma_1+\#\Gamma_3) + e^{-i(\mathbf{b}_1+\mathbf{b}_2)\cdot\mathbf{r}_0}(\#M_1+\#M_3) + (e^{-i\mathbf{b}_1\cdot\mathbf{r}_0}+e^{-i\mathbf{b}_2\cdot\mathbf{r}_0})\#X_1)\\ &\quad - i((\#\Gamma_2+\#\Gamma_4) + e^{-i(\mathbf{b}_1+\mathbf{b}_2)\cdot\mathbf{r}_0}(\#M_2+\#M_4) + (e^{-i\mathbf{b}_1\cdot\mathbf{r}_0}+e^{-i\mathbf{b}_2\cdot\mathbf{r}_0})\#X_2)\\ &= i(1+e^{-i\mathbf{b}_1\cdot\mathbf{r}_0}+e^{-i\mathbf{b}_2\cdot\mathbf{r}_0}+e^{-i(\mathbf{b}_1+\mathbf{b}_2)\cdot\mathbf{r}_0})(\#\Gamma_1+\#\Gamma_3) + ie^{-i(\mathbf{b}_1+\mathbf{b}_2)\cdot\mathbf{r}_0}([M_1]+[M_3]) + i(e^{-i\mathbf{b}_1\cdot\mathbf{r}_0}+e^{-i\mathbf{b}_2\cdot\mathbf{r}_0})[X_1]\\ &\quad - i(1+e^{-i\mathbf{b}_1\cdot\mathbf{r}_0}+e^{-i\mathbf{b}_2\cdot\mathbf{r}_0}+e^{-i(\mathbf{b}_1+\mathbf{b}_2)\cdot\mathbf{r}_0})(\#\Gamma_2+\#\Gamma_4) - ie^{-i(\mathbf{b}_1+\mathbf{b}_2)\cdot\mathbf{r}_0}([M_2]+[M_4]) - i(e^{-i\mathbf{b}_1\cdot\mathbf{r}_0}+e^{-i\mathbf{b}_2\cdot\mathbf{r}_0})[X_2]\\ &= 2i\left\{\left(\frac{1+e^{-i\mathbf{b}_1\cdot\mathbf{r}_0}+e^{-i\mathbf{b}_2\cdot\mathbf{r}_0}+e^{-i(\mathbf{b}_1+\mathbf{b}_2)\cdot\mathbf{r}_0}}{2}\right)(\#\Gamma_1+\#\Gamma_3-\#\Gamma_2-\#\Gamma_4)\right.\\ &\quad \left. + e^{-i(\mathbf{b}_1+\mathbf{b}_2)\cdot\mathbf{r}_0}([M_1]-[M_2]) + (e^{-i\mathbf{b}_1\cdot\mathbf{r}_0}+e^{-i\mathbf{b}_2\cdot\mathbf{r}_0})[X]\right\},\end{aligned} \tag{A54}$$

where we used $[X] \equiv [X_1] = -[X_2]$ due to particle-hole symmetry as well. By evaluating these expressions at the rotation centers $\mathbf{r}_0 = \mathbf{a}_1, \mathbf{a}_1+\mathbf{a}_2$, we obtain

$$T_{\mathcal{S}}^{c(2)}\big|_{\mathbf{r}_0=\mathbf{a}_1} = -2i([M_1]-[M_2]), \tag{A55}$$

$$T_{\mathcal{S}}^{c(2)}\big|_{\mathbf{r}_0=\mathbf{a}_1+\mathbf{a}_2} = 2i\{([M_1]-[M_2]) - 2[X]\}, \tag{A56}$$

$$T_{\mathcal{S}}^{c(4)}\big|_{\mathbf{r}_0=\mathbf{a}_1+\mathbf{a}_2} = -i\sqrt{2}([M_1]+[M_2]), \tag{A57}$$

which finally implies, using Eq. (A48), that

$$[X] = \frac{i}{4}\left(T_{\mathcal{S}}^{c(2)}\big|_{\mathbf{r}_0=\mathbf{a}_1} + T_{\mathcal{S}}^{c(2)}\big|_{\mathbf{r}_0=\mathbf{a}_1+\mathbf{a}_2}\right)$$

$$= \frac{i}{4}\mathrm{Tr}\left[\left(\bar{c}_{\mathcal{S}}^{(2)}\big|_{\mathbf{r}_0=\mathbf{a}_1}\right) + \left(\bar{c}_{\mathcal{S}}^{(2)}\big|_{\mathbf{r}_0=\mathbf{a}_1+\mathbf{a}_2}\right)\right], \tag{A58}$$

$$[M_{1,2}] = \frac{i}{4}\left(\sqrt{2}T_{\mathcal{S}}^{c(4)}\big|_{\mathbf{r}_0=\mathbf{a}_1+\mathbf{a}_2} \pm T_{\mathcal{S}}^{c(2)}\big|_{\mathbf{r}_0=\mathbf{a}_1}\right)$$

$$= \frac{i}{4}\mathrm{Tr}\left[\sqrt{2}\left(\bar{c}_{\mathcal{S}}^{(4)}|_{\mathbf{r}_0=\mathbf{a}_1+\mathbf{a}_2}\right) \pm \left(\bar{c}_{\mathcal{S}}^{(2)}|_{\mathbf{r}_0=\mathbf{a}_1}\right)\right], \tag{A59}$$

which are the expressions discussed in the main text. The topological marker for this invariant satisfies

$$\left|\mathcal{T}_{\mathcal{S}}^{c(n)}(\mathbf{r})\right| < O(e^{-2\sin[\frac{\pi}{n}]|\mathbf{r}-\mathcal{S}|/\zeta}). \tag{A60}$$

When $\zeta \ll |x-\mathcal{S}|$ and an impurity placed at $\mathbf{r}=\mathbf{R}_0$ will change an invariant centered at $\mathcal{S}$ by an exponentially small amount

$$\left|T_{\mathcal{S}}^{c(n)'}(\mathbf{R}_0) - T_{\mathcal{S}}^{c(n)}\right| < O\left(e^{-2\sin\left[\frac{\pi}{n}\right]|\mathbf{R}_0-\mathcal{S}|/\zeta}\right), \tag{A61}$$

when $\zeta \ll |\mathbf{R}_0-\mathcal{S}|$ where the notation $|\mathbf{R}_0-\mathcal{S}|$ means the shortest distance to any of the invariant points in the set $\mathcal{S}$.

4. Mirror-symmetric DIII topological superconductors in two dimensions

a. Conventional classification

In the main text, we discussed the basis-independent approach to the classification of mirror-symmetric DIII topological superconductors in two dimensions. Here, we will make contact with the momentum-space classification in order to connect with Eq. (A20).

As we mentioned in the main text, a 2D mirror-symmetric superconductor in class DIII is described by a Bogoliubov–de Gennes Hamiltonian $\hat{H}$ such that $[\hat{m}_{\mathcal{S}},\hat{H}]=0$. The mirror-invariant lines are located at $\mathcal{S}=(Y_1+y_0, Y_2+y_0)$, with $y_0=0,\frac{1}{2}$. We focus on the case when $\hat{m}_{\mathcal{S}}^2=-1$. If we Fourier transform only the coordinate that changes under mirror symmetry, the mirror constraint on the Bloch Hamiltonian is

$$\widetilde{m}_{\mathcal{S}}(k_y)h(k_y)\widetilde{m}_{\mathcal{S}}^{-1}(k_y) = h(-k_y), \tag{A62}$$

where $\widetilde{m}_{\mathcal{S}}(k_y)$ is the momentum representation of the mirror operator. At the mirror-invariant momentum lines $k_y^{\text{inv}}=0,\pi$, the Bloch states can be labeled with mirror eigenvalues. By using the chiral symmetry $\chi=TC$ that arises from having both time-reversal T and particle-hole C symmetries, one can define topologically invariant mirror-winding numbers given by [44]

$$\nu_{\mathcal{S}}^{(\pm)}\left(k_y^{\text{inv}}\right) = -\frac{1}{N_x}\text{Tr}[(S_-\mathcal{Q}_{\pm,k_y^{\text{inv}}}S_+)[\hat{X},(S_+\mathcal{Q}_{\pm,k_y^{\text{inv}}}S_-)]], \tag{A63}$$

where $\mathcal{Q}_{\pm,k_y^{\text{inv}}}=2\mathcal{P}_{\pm,k_y^{\text{inv}}}-\mathbb{I}$, $S_\pm=(\mathbb{I}\pm\hat{\chi})/2$ projects into chiral subspaces with eigenvalue $\chi=\pm1$, and $\mathcal{P}_{\pm,k_y^{\text{inv}}}$ is the projection operator into the occupied states with mirror eigenvalue $\pm i$. Due to time-reversal symmetry, $\nu_{\mathcal{S}}^{(+)}(k_y^{\text{inv}}) = -\nu_{\mathcal{S}}^{(-)}(k_y^{\text{inv}})$. The integers at the two invariant momenta lead to the known $\mathbb{Z}\times\mathbb{Z}$ classification [12]. To express the winding in terms explicitly of projection operators, we write

$$\begin{aligned}
\nu_{\mathcal{S}}^{(\pm)}(k_y^{\text{inv}}) &= -\frac{1}{N_x}\text{Tr}\left[\left(S_-\mathcal{Q}_{\pm,k_y^{\text{inv}}}S_+\right)\left[\hat{X},\left(S_+\mathcal{Q}_{\pm,k_y^{\text{inv}}}S_-\right)\right]\right] && \text{(A64)}\\
&= -\frac{1}{N_x}\text{Tr}\left[\left(2\mathcal{P}_{\pm,k_y^{\text{inv}}}-\mathbb{I}\right)S_+\left[\hat{X},\left(2\mathcal{P}_{\pm,k_y^{\text{inv}}}-\mathbb{I}\right)\right]S_-\right] && \text{(A65)}\\
&= -\frac{4}{N_x}\text{Tr}\left[\mathcal{P}_{\pm,k_y^{\text{inv}}}\left[\hat{X},S_+\mathcal{P}_{\pm,k_y^{\text{inv}}}S_-\right]\right] && \text{(A66)}\\
&= -\frac{4}{N_x}\text{Tr}\left[\mathcal{P}_{\pm,k_y^{\text{inv}}}\left[\hat{X},\left(\frac{(\mathbb{I}+\hat{\chi})}{2}\right)\mathcal{P}_{\pm,k_y^{\text{inv}}}\left(\frac{(\mathbb{I}-\hat{\chi})}{2}\right)\right]\right] && \text{(A67)}\\
&= -\frac{1}{N_x}\text{Tr}\left[\mathcal{P}_{\pm,k_y^{\text{inv}}}\left[\hat{X},\mathcal{P}_{\pm,k_y^{\text{inv}}}+\hat{\chi}\mathcal{P}_{\pm,k_y^{\text{inv}}}-\mathcal{P}_{\pm,k_y^{\text{inv}}}\hat{\chi}-\hat{\chi}\mathcal{P}_{\pm,k_y^{\text{inv}}}\hat{\chi}\right]\right] && \text{(A68)}\\
&= -\frac{1}{N_x}\text{Tr}\left[\mathcal{P}_{\pm,k_y^{\text{inv}}}\left[\hat{X},\mathcal{P}_{\pm,k_y^{\text{inv}}}+\left(\hat{\chi}-\mathcal{P}_{\pm,k_y^{\text{inv}}}\hat{\chi}\right)-\mathcal{P}_{\pm,k_y^{\text{inv}}}\hat{\chi}-\left(\mathbb{I}-\mathcal{P}_{\pm,k_y^{\text{inv}}}\right)\right]\right] && \text{(A69)}\\
&= -\frac{2}{N_x}\text{Tr}\left[\mathcal{P}_{\pm,k_y^{\text{inv}}}\left[\hat{X},\mathcal{P}_{\pm,k_y^{\text{inv}}}\right]\right]+\frac{2}{N_x}\text{Tr}\left[\mathcal{P}_{\pm,k_y^{\text{inv}}}\left[\hat{X},\mathcal{P}_{\pm,k_y^{\text{inv}}}\hat{\chi}\right]\right] && \text{(A70)}\\
&= \frac{2}{N_x}\text{Tr}\left[\mathcal{P}_{\pm,k_y^{\text{inv}}}\left[\hat{X},\mathcal{P}_{\pm,k_y^{\text{inv}}}\right]\hat{\chi}\right], && \text{(A71)}
\end{aligned}$$

which is the expression we presented in the main text.

b. Basis-independent classification

We now implement Eq. (A20) for this TCP. As is clear from the previous section, the topological invariants of the invariant subspaces are

$$\tau_{\mathcal{S},b}^{\pm}\left(k_y^{\text{inv}}\right) = \nu_{\mathcal{S}}^{\pm}\left(k_y^{\text{inv}}\right), \tag{A72}$$

where we added the index b to be reminded that it refers to the bulk invariant, as opposed to the edge invariant that we introduce in the next subsection. Furthermore, we have that

$$\mathcal{F}(\mathcal{P}) = 2N_x^{-1}\mathcal{P}[\hat{X},\mathcal{P}]\chi. \tag{A73}$$

By applying Eq. (A20), we then have the topological invariants

$$\begin{aligned}
T_{\mathcal{S}}^{m} &= \sum_{k_y^{\text{inv}}}\left[(+i)\nu_{\mathcal{S}}^{+}\left(k_y^{\text{inv}}\right)+(-i)\nu_{\mathcal{S}}^{-}\left(k_y^{\text{inv}}\right)\right]\\
&= \text{Tr}[\overline{m}_{\mathcal{S}}\mathcal{F}(\mathcal{P}_G)]. && \text{(A74)}
\end{aligned}$$

The relation with the invariant we defined in the main text is then

$$\mathcal{V}^m_{\mathcal{S}} = -\frac{i}{2} T^m_{\mathcal{S}}. \tag{A75}$$

The topological marker for this invariant satisfies

$$\left|\mathcal{T}^m_{\mathcal{S}}(y)\right| < O(e^{-2|y-\mathcal{S}|/\zeta}), \tag{A76}$$

when $\zeta \ll |y-\mathcal{S}|$ and an impurity placed at $y = Y_0$ will change an invariant centered at $\mathcal{S}$ by an exponentially small amount

$$\left|T^{m'}_{\mathcal{S}}(Y_0) - T^m_{\mathcal{S}}\right| < O(e^{-2|Y_0-\mathcal{S}|/\zeta}) \tag{A77}$$

when $\zeta \ll |Y_0 - \mathcal{S}|$.

c. Integer topological invariants for the edge

In the main text, we used the bulk-boundary relation $\Delta^m_{\mathcal{S}} = -\frac{i}{2}\mathrm{Tr}[\overline{m}^{\mathrm{edge}}_{\mathcal{S}}\chi] = \mathcal{V}^m_{\mathcal{S}}$, which we will now prove in this section. To do this, we begin by noting that we can write $\Delta^m_{\mathcal{S}}$ in the suggestive form

$$\Delta^m_{\mathcal{S}} = -\frac{i}{2}\mathrm{Tr}[\overline{m}_{\mathcal{S}}\mathcal{F}(\mathcal{P}_{\mathrm{edge}})], \tag{A78}$$

which has the form of the invariants in Eq. (A20), in this case with the function $\mathcal{F}(\mathcal{P}) = \mathcal{P}\chi$. Thus, in momentum space we must obtain that $\Delta^m_{\mathcal{S}}$ receives contribution exclusively from the invariant momenta in the form

$$\Delta^m_{\mathcal{S}} = \left(-\frac{i}{2}\right)\sum_{k^{\mathrm{inv}}_y}\left[(+i)\tau^{\mathrm{edge}}_+\left(k^{\mathrm{inv}}_y\right) + (-i)\tau^{\mathrm{edge}}_-\left(k^{\mathrm{inv}}_y\right)\right], \tag{A79}$$

where we defined new edge topological invariants

$$\begin{aligned}\tau^{\mathrm{edge}}_m\left(k^{\mathrm{inv}}_y\right) &\equiv \mathrm{Tr}\left[\mathcal{P}_{\mathrm{edge}}\left(k^{\mathrm{inv}}_y\right)\mathcal{F}\left(\mathcal{P}_{\mathrm{edge}}\left(k^{\mathrm{inv}}_y\right)\right)\right] \\ &= \mathrm{Tr}\left[\mathcal{P}_{\mathrm{edge}}\left(k^{\mathrm{inv}}_y\right)\chi\right],\end{aligned} \tag{A80}$$

with $\mathcal{P}_{\mathrm{edge}}(k^{\mathrm{inv}}_y)$ the projector onto the boundary states with momentum k^{inv}_y and mirror eigenvalue mi. Because of the form of the function $\mathcal{F}$ in this case, the quantities $\tau^{\mathrm{edge}}_m(k^{\mathrm{inv}}_y)$ count the difference

$$\begin{aligned}\mathrm{Tr}\left[\mathcal{P}_{\mathrm{edge}}\left(k^{\mathrm{inv}}_y\right)\chi\right] &= \sum_{n\in\mathrm{edge}}\left\langle u^n_{k^{\mathrm{inv}}_y}\middle|\chi\middle|u^n_{k^{\mathrm{inv}}_y}\right\rangle \\ &= \mathcal{N}^m_+\left(k^{\mathrm{inv}}_y\right) - \mathcal{N}^m_-\left(k^{\mathrm{inv}}_y\right)\end{aligned} \tag{A81}$$

at the invariant momentum k^{inv}_y in a given mirror subspace m, with $\mathcal{N}^m_\chi(k^{\mathrm{inv}}_y)$ the number of modes with chiral eigenvalue $\chi = \pm 1$. Due to the bulk-boundary correspondence of AIII systems, this difference must be equal to the bulk topological winding (A71), and thus

$$\tau^{\mathrm{edge}}_m\left(k^{\mathrm{inv}}_y\right) = \nu^{(m)}_{\mathcal{S}}\left(k^{\mathrm{inv}}_y\right). \tag{A82}$$

Finally, putting together Eqs. (A75), (A79), and (A82), we obtain the relation

$$\begin{aligned}\Delta^m_{\mathcal{S}} &= \frac{1}{2}\sum_{k^{\mathrm{inv}}_y}\left[\tau^{\mathrm{edge}}_+\left(k^{\mathrm{inv}}_y\right) - \tau^{\mathrm{edge}}_-\left(k^{\mathrm{inv}}_y\right)\right] \\ &= \frac{1}{2}\sum_{k^{\mathrm{inv}}_y}\left[\nu^{(+)}_{\mathcal{S}}\left(k^{\mathrm{inv}}_y\right) - \nu^{(-)}_{\mathcal{S}}\left(k^{\mathrm{inv}}_y\right)\right] = \mathcal{V}^m_{\mathcal{S}}\end{aligned} \tag{A83}$$

as we had set out to prove.

d. Quantized edge shift of gapless Majorana boundary modes

In this section, we derive Eq. (7) from the main text, which relates the local edge shift $\delta\mathcal{Y}^\chi_{\mathrm{edge}}(R_1)$ with the bulk invariant $\mathcal{V}^m_{\mathcal{S}}$. Consider the projected position operator $\mathcal{W}^\chi_{\mathrm{edge}} = \mathcal{P}^\chi_{\mathrm{edge}} e^{-2\pi i\hat{Y}/L_y}\mathcal{P}^\chi_{\mathrm{edge}}$. We denote its eigenvalues and eigenstates by $\{e^{-2\pi i\lambda_{R_y j}/L_y}\}$ and $\{|\Psi^\chi_{R_y j}\rangle\}$, respectively. Here, R_y labels unit cells along the edge, and $j = 1, \ldots, N_b$, where N_b is the number of subbands included in the detached Majorana band (DMB). Thus, the number of states in the edge projector $\mathcal{P}_{\mathrm{edge}}$ is $N_b L_y$. Let us write $\lambda_{R_y j} = R_y + \nu_{R_y j}$. The edge shift is then defined by

$$\delta\mathcal{Y}^\chi_{\mathrm{edge}}(R_1) = \left(\sum_{j=1}^{N_b}\nu_{R_1 j}\right)\mathrm{mod}\ 1. \tag{A84}$$

Now, mirror symmetry imposes the constraint

$$\begin{aligned}\hat{m}_{\mathcal{S}}\mathcal{W}^\chi_{\mathrm{edge}}\hat{m}^{-1}_{\mathcal{S}} &= \mathcal{P}^\chi_{\mathrm{edge}}\hat{m}_{\mathcal{S}}e^{-2\pi i\hat{Y}/L_y}\hat{m}^{-1}_{\mathcal{S}}\mathcal{P}^\chi_{\mathrm{edge}} \\ &= e^{-4\pi i S/L_y}\left(\mathcal{W}^\chi_{\mathrm{edge}}\right)^\dagger.\end{aligned} \tag{A85}$$

Thus, we have that $\mathcal{W}^\chi_{\mathrm{edge}}|\Psi^\chi_{R_y j}\rangle = e^{-2\pi i\lambda_{R_y j}/L_y}|\Psi^\chi_{R_y j}\rangle$ implies $\mathcal{W}^\chi_{\mathrm{edge}}\hat{m}_{\mathcal{S}}|\Psi^\chi_{R_y j}\rangle = e^{-2\pi i(2S-\lambda_{R_y j})/L_y}\hat{m}_{\mathcal{S}}|\Psi^\chi_{R_y j}\rangle$. Because of this constraint, for a given fixed unit cell R_y, there are three types of Wannier centers $\nu_{R_y j}$:

(1) Those that come in symmetry-related pairs $\{\nu_{R_y j}\mathrm{mod}\ 1, -\nu_{R_y j}\mathrm{mod}\ 1\}$.

(2) Those that coincide with an integer mirror-invariant point $\nu_{R_y j}\mathrm{mod}\ 1 = 0$.

(3) Those that coincide with a half-integer mirror-invariant point $\nu_{R_y j}\mathrm{mod}\ 1 = \frac{1}{2}$.

In view of these possibilities, if we denote by $N_{\chi,1/2}(R_1)$ the number of Wannier states centered at $R_1 + \frac{1}{2}$, then

$$\begin{aligned}\delta\mathcal{Y}^\chi_{\mathrm{edge}}(R_1) &= \left(\sum_{j=1}^{N_b}\lambda_{R_1 j}\right)\mathrm{mod}\ 1 \\ &= \left(\sum_{i=1}^{N_{\chi,1/2}}\frac{1}{2}\right)\mathrm{mod}\ 1 \\ &= \left[\frac{1}{2}N_{\chi,1/2}(R_1)\right]\mathrm{mod}\ 1.\end{aligned} \tag{A86}$$

Thus, the only way to obtain a nonzero shift $\delta\mathcal{Y}^\chi_{\mathrm{edge}}(R_1) = \frac{1}{2}$ is for there to be an odd number of Wannier centers at the midpoint of the unit cell R_1. Next, let us write $N_{\chi,1/2}(R_1) = N^{(+)}_{\chi,1/2}(R_1) + N^{(-)}_{\chi,1/2}(R_1)$, where $N^{(\pm)}_{\chi,1/2}(R_1)$ is the number of

Wannier states centered at $R_1 + \frac{1}{2}$ with $\pm i$ mirror eigenvalues. Then

$$\begin{aligned}\delta\mathcal{Y}^{\chi}_{\text{edge}}(R_1) &= \left[\tfrac{1}{2}(N^{(+)}_{\chi,1/2}(R_1) + N^{(-)}_{\chi,1/2}(R_1))\right]\text{mod } 1 \\ &= \left[\tfrac{1}{2}(N^{(+)}_{\chi,1/2}(R_1) - N^{(-)}_{\chi,1/2}(R_1))\right]\text{mod } 1. \quad \text{(A87)}\end{aligned}$$

Consider the set of mirror-invariant points $S|_{y_0=1/2} = \{R_1 + \frac{1}{2}, R_2 + \frac{1}{2}\}$. Due to the constraint of mirror symmetry, for $\lambda_{R_y j} \neq R_1 + \frac{1}{2}$, the state $|\Psi^{\chi}_{R_y j}\rangle$ is orthogonal to the state $\hat{m}_{\mathcal{S}}|\Psi^{\chi}_{R_y j}\rangle$. By contrast, if $\lambda_{R_y j} = R_1 + \frac{1}{2}$, then $|\Psi^{\chi}_{R_y j}\rangle$ is an eigenstate of $\hat{m}_{\mathcal{S}}|_{y_0=1/2}$. It follows that

$$N^{(+)}_{\chi,1/2}(R_1) - N^{(-)}_{\chi,1/2}(R_1) = -\frac{i}{2}\sum_{R_y j}\left\langle\Psi^{\chi}_{R_y j}\right|(\hat{m}_{\mathcal{S}}|_{y_0=1/2})\left|\Psi^{\chi}_{R_y j}\right\rangle. \quad \text{(A88)}$$

Note that the dependence of the right-hand side on R_1 comes from the index $S|_{y_0=1/2}$ of the mirror operator that is chosen. The factor of $\frac{1}{2}$ is due to the fact that the sum counts the *two* points in $S|_{y_0=1/2}$, and we defined $N_{\chi,1/2}$ with respect to only *one* of them. Using Eq. (A88) in (A87), we then obtain

$$\delta\mathcal{Y}^{\chi}_{\text{edge}}(R_1) = \left[-\frac{i}{4}\sum_{R_y j}\left\langle\Psi^{\chi}_{R_y j}\right|(\hat{m}_{\mathcal{S}}|_{y_0=1/2})\left|\Psi^{\chi}_{R_y j}\right\rangle\right]\text{mod } 1. \quad \text{(A89)}$$

Now, note that since $\hat{\chi}T|\Psi^{+}_{R_y j}\rangle = -\chi T|\Psi^{+}_{R_y j}\rangle$ then $T|\Psi^{+}_{R_y j}\rangle \propto |\Psi^{-}_{R_y j}\rangle$. Thus, if $\hat{m}_{\mathcal{S}}|_{y_0=1/2}|\Psi^{+}_{R_y j}\rangle = e^{i\phi}|\Psi^{+}_{R_y j}\rangle$, then by acting with T on both sides we obtain $\hat{m}_{\mathcal{S}}|_{y_0=1/2}|\Psi^{-}_{R_y j}\rangle = e^{-i\phi}|\Psi^{-}_{R_y j}\rangle$, i.e., the two states $|\Psi^{+}_{R_y j}\rangle$ and $|\Psi^{-}_{R_y j}\rangle$ have opposite mirror eigenvalues. Because of this, we can write

$$\begin{aligned}&\left\langle\Psi^{\chi}_{R_y j}\right|(\hat{m}_{\mathcal{S}}|_{y_0=1/2})\left|\Psi^{\chi}_{R_y j}\right\rangle \\ &\quad= \tfrac{1}{2}\left(\left\langle\Psi^{+}_{R_y j}\right|(\hat{m}_{\mathcal{S}}|_{y_0=1/2})\left|\Psi^{+}_{R_y j}\right\rangle\right. \\ &\quad\quad\left. - \left\langle\Psi^{-}_{R_y j}\right|(\hat{m}_{\mathcal{S}}|_{y_0=1/2})\left|\Psi^{-}_{R_y j}\right\rangle\right). \quad \text{(A90)}\end{aligned}$$

We then obtain

$$\begin{aligned}\delta\mathcal{Y}^{\chi}_{\text{edge}}(R_1) = \Bigg[-\frac{i}{8}\sum_{R_y j}\Big\{&\left\langle\Psi^{+}_{R_y j}\right|(\hat{m}_{\mathcal{S}}|_{y_0=1/2})\left|\Psi^{+}_{R_y j}\right\rangle \\ &- \left\langle\Psi^{-}_{R_y j}\right|(\hat{m}_{\mathcal{S}}|_{y_0=1/2})\left|\Psi^{-}_{R_y j}\right\rangle\Big\}\Bigg]\text{mod } 1. \quad \text{(A91)}\end{aligned}$$

Finally, we replace the sum over Wannier functions by a trace over the full Hilbert space of the system by introducing the projection operator $\mathcal{P}_{\text{edge}}$:

$$\begin{aligned}\delta\mathcal{Y}^{\chi}_{\text{edge}}(R_1) &= \left[-\frac{i}{8}\sum_{R_y j\chi}\left\langle\Psi^{\chi}_{R_y j}\right|(\hat{m}_{\mathcal{S}}|_{y_0=1/2})\hat{\chi}\left|\Psi^{\chi}_{R_y j}\right\rangle\right]\text{mod } 1 \\ &= \left[-\frac{i}{8}\text{Tr}[\mathcal{P}_{\text{edge}}(\hat{m}_{\mathcal{S}}|_{y_0=1/2})\hat{\chi}]\right]\text{mod } 1 \quad \text{(A92)} \\ &= \left[\frac{1}{4}\Delta^{m}_{\mathcal{S}}\big|_{y_0=1/2}\right]\text{mod}1, \\ &= \left[\frac{1}{4}\mathcal{V}^{m}_{\mathcal{S}}\big|_{y_0=1/2}\right]\text{mod } 1, \quad \text{(A93)}\end{aligned}$$

which is the expression we discussed in the main text.

e. Constructing the projection operator for the DMB

As we state in the main text, to obtain the edge projector $\mathcal{P}_{\text{edge}}$ of the boundary bands of *only one* of the edges, we gap out the boundary modes on the opposite edge. To achieve this, we add the term

$$\begin{aligned}V = &\sum_{k_y}\alpha(f_1\tau_3\sigma_0)|x = 1, k_y\rangle\langle x = 1, k_y| \\ &+ \beta(f_1\tau_3\sigma_1 - \cos k_y f_0\tau_2\sigma_0)|x = L_x, k_y\rangle\langle x = L_x, k_y|, \quad \text{(A94)}\end{aligned}$$

with $\alpha = -1.0$, $\beta = 0.5$ for the weak TCP example. For the mirror-topological TCP, we use

$$\begin{aligned}V = &\sum_{k_y}\alpha(f_1\tau_3\sigma_0)|x = 1, k_y\rangle\langle x = 1, k_y| \\ &+ \beta(f_0\tau_3\sigma_1)|x = L_x, k_y\rangle\langle x = L_x, k_y|, \quad \text{(A95)}\end{aligned}$$

with $\alpha = 0.1$, $\beta = -0.8$.

[1] M. Z. Hasan and C. L. Kane, *Colloquium:* Topological insulators, Rev. Mod. Phys. **82**, 3045 (2010).

[2] X.-L. Qi and S.-C. Zhang, Topological insulators and superconductors, Rev. Mod. Phys. **83**, 1057 (2011).

[3] L. Fu, Topological crystalline insulators, Phys. Rev. Lett. **106**, 106802 (2011).

[4] T. H. Hsieh, H. Lin, J. Liu, W. Duan, A. Bansil, and L. Fu, Topological crystalline insulators in the SnTe material class, Nat. Commun. **3**, 982 (2012).

[5] S.-Y. Xu, C. Liu, N. Alidoust, M. Neupane, D. Qian, I. Belopolski, J. D. Denlinger, Y. J. Wang, H. Lin, L. A. Wray, G. Landolt, B. Slomski, J. H. Dil, A. Marcinkova, E. Morosan, Q. Gibson, R. Sankar, F. C. Chou, R. J. Cava, A. Bansil *et al.*, Observation of a topological crystalline insulator phase and topological phase transition in Pb_{1-x} Sn_x Te, Nat. Commun. **3**, 1192 (2012).

[6] P. Dziawa, B. J. Kowalski, K. Dybko, R. Buczko, A. Szczerbakow, M. Szot, E. Łusakowska, T. Balasubramanian, B. M. Wojek, M. H. Berntsen, O. Tjernberg, and T. Story, Topological crystalline insulator states in $Pb_{1-x}Sn_x$ Se, Nat. Mater. **11**, 1023 (2012).

[7] Y. Tanaka, Z. Ren, T. Sato, K. Nakayama, S. Souma, T. Takahashi, K. Segawa, and Y. Ando, Experimental realization

of a topological crystalline insulator in SnTe, Nat. Phys. **8**, 800 (2012).

[8] Y. Okada, M. Serbyn, H. Lin, D. Walkup, W. Zhou, C. Dhital, M. Neupane, S. Xu, Y. J. Wang, R. Sankar, F. Chou, A. Bansil, M. Z. Hasan, S. D. Wilson, L. Fu, and V. Madhavan, Observation of dirac node formation and mass acquisition in a topological crystalline insulator, Science **341**, 1496 (2013).

[9] T. L. Hughes, E. Prodan, and B. A. Bernevig, Inversion-symmetric topological insulators, Phys. Rev. B **83**, 245132 (2011).

[10] C. Fang, M. J. Gilbert, and B. A. Bernevig, Bulk topological invariants in noninteracting point group symmetric insulators, Phys. Rev. B **86**, 115112 (2012).

[11] C.-K. Chiu, H. Yao, and S. Ryu, Classification of topological insulators and superconductors in the presence of reflection symmetry, Phys. Rev. B **88**, 075142 (2013).

[12] F. Zhang, C. L. Kane, and E. J. Mele, Topological mirror superconductivity, Phys. Rev. Lett. **111**, 056403 (2013).

[13] C. Fang, M. J. Gilbert, and B. A. Bernevig, New class of topological superconductors protected by magnetic group symmetries, Phys. Rev. Lett. **112**, 106401 (2014).

[14] A. Alexandradinata, C. Fang, M. J. Gilbert, and B. A. Bernevig, Spin-orbit-free topological insulators without time-reversal symmetry, Phys. Rev. Lett. **113**, 116403 (2014).

[15] J. C. Y. Teo and T. L. Hughes, Existence of majorana-fermion bound states on disclinations and the classification of topological crystalline superconductors in two dimensions, Phys. Rev. Lett. **111**, 047006 (2013).

[16] Wladimir A. Benalcazar, J. C. Y. Teo, and T. L. Hughes, Classification of two-dimensional topological crystalline superconductors and Majorana bound states at disclinations, Phys. Rev. B **89**, 224503 (2014).

[17] H. Yao and S. Ryu, Interaction effect on topological classification of superconductors in two dimensions, Phys. Rev. B **88**, 064507 (2013).

[18] H. Isobe and L. Fu, Theory of interacting topological crystalline insulators, Phys. Rev. B **92**, 081304(R) (2015).

[19] Y. Qi and L. Fu, Anomalous crystal symmetry fractionalization on the surface of topological crystalline insulators, Phys. Rev. Lett. **115**, 236801 (2015).

[20] C.-K. Chiu, D. I. Pikulin, and M. Franz, Proposed platform to study interaction-enabled topological phases with fermionic particles, Phys. Rev. B **92**, 241115(R) (2015).

[21] M. F. Lapa, J. C. Y. Teo, and T. L. Hughes, Interaction-enabled topological crystalline phases, Phys. Rev. B **93**, 115131 (2016).

[22] H. Song, S.-J. Huang, L. Fu, and M. Hermele, Topological phases protected by point group symmetry, Phys. Rev. X **7**, 011020 (2017).

[23] B. Bradlyn, L. Elcoro, J. Cano, M. G. Vergniory, Z. Wang, C. Felser, M. I. Aroyo, and B. A. Bernevig, Topological quantum chemistry, Nature (London) **547**, 298 (2017).

[24] J. Cano, B. Bradlyn, Z. Wang, L. Elcoro, M. G. Vergniory, C. Felser, M. I. Aroyo, and B. A. Bernevig, Building blocks of topological quantum chemistry: Elementary band representations, Phys. Rev. B **97**, 035139 (2018).

[25] W. A. Benalcazar, B. A. Bernevig, and T. L. Hughes, Quantized electric multipole insulators, Science **357**, 61 (2017).

[26] W. A. Benalcazar, B. A. Bernevig, and T. L. Hughes, Electric multipole moments, topological multipole moment pumping, and chiral hinge states in crystalline insulators, Phys. Rev. B **96**, 245115 (2017).

[27] F. Schindler, A. M. Cook, M. G. Vergniory, Z. Wang, S. S. P. Parkin, B. A. Bernevig, and T. Neupert, Higher-order topological insulators, Sci. Adv. **4**, eaat0346 (2018).

[28] L. Fu and C. L. Kane, Topology, delocalization via average symmetry and the symplectic Anderson transition, Phys. Rev. Lett. **109**, 246605 (2012).

[29] I. C. Fulga, B. van Heck, J. M. Edge, and A. R. Akhmerov, Statistical topological insulators, Phys. Rev. B **89**, 155424 (2014).

[30] J. Song and E. Prodan, Quantization of topological invariants under symmetry-breaking disorder, Phys. Rev. B **92**, 195119 (2015).

[31] I. Zeljkovic, Y. Okada, M. Serbyn, R. Sankar, D. Walkup, W. Zhou, J. Liu, G. Chang, Y. J. Wang, M. Z. Hasan, F. Chou, H. Lin, A. Bansil, L. Fu, and V. Madhavan, Dirac mass generation from crystal symmetry breaking on the surfaces of topological crystalline insulators, Nat. Mater. **14**, 318 (2015).

[32] M. Diez, D. I. Pikulin, I. C. Fulga, and J. Tworzydlo, Extended topological group structure due to average reflection symmetry, New J. Phys. **17**, 043014 (2015).

[33] C. Fang, M. J. Gilbert, and B. A. Bernevig, Entanglement spectrum classification of C_n-invariant noninteracting topological insulators in two dimensions, Phys. Rev. B **87**, 035119 (2013).

[34] R. Bianco and R. Resta, Mapping topological order in coordinate space, Phys. Rev. B **84**, 241106(R) (2011).

[35] E. J. Meier, F. A. An, A. Dauphin, M. Maffei, P. Massignan, T. L. Hughes, and B. Gadway, Observation of the topological Anderson insulator in disordered atomic wires, Science **362**, 929 (2018).

[36] J. Sykes and R. Barnett, Local topological markers in odd dimensions, Phys. Rev. B **103**, 155134 (2021).

[37] J. D. Hannukainen, M. F. Martínez, J. H. Bardarson, and T. K. Kvorning, Local topological markers in odd spatial dimensions and their application to amorphous topological matter, Phys. Rev. Lett. **129**, 277601 (2022).

[38] W. Chen, Universal topological marker, Phys. Rev. B **107**, 045111 (2023).

[39] S.-J. Huang, H. Song, Y.-P. Huang, and M. Hermele, Building crystalline topological phases from lower-dimensional states, Phys. Rev. B **96**, 205106 (2017).

[40] Z. Song, C. Fang, and Y. Qi, Real-space recipes for general topological crystalline states, Nat. Commun. **11**, 4197 (2020).

[41] K. Shiozaki, H. Shapourian, and S. Ryu, Many-body topological invariants in fermionic symmetry-protected topological phases: Cases of point group symmetries, Phys. Rev. B **95**, 205139 (2017).

[42] H. Shapourian, K. Shiozaki, and S. Ryu, Many-body topological invariants for fermionic symmetry-protected topological phases, Phys. Rev. Lett. **118**, 216402 (2017).

[43] K. Shiozaki, H. Shapourian, K. Gomi, and S. Ryu, Many-body topological invariants for fermionic short-range entangled topological phases protected by antiunitary symmetries, Phys. Rev. B **98**, 035151 (2018).

[44] I. Mondragon-Shem, T. L. Hughes, J. Song, and E. Prodan, Topological criticality in the chiral-symmetric AIII class at strong disorder, Phys. Rev. Lett. **113**, 046802 (2014).

[45] S. Kivelson, Wannier functions in one-dimensional disordered systems: Application to fractionally charged solitons, Phys. Rev. B **26**, 4269 (1982).

[46] Z. Wang and S.-C. Zhang, Simplified topological invariants for interacting insulators, Phys. Rev. X **2**, 031008 (2012).

[47] W. Zhang and L.-M. Duan, Tomography of correlation functions for ultracold atoms via time-of-flight images, Phys. Rev. A **80**, 063614 (2009).

[48] E. Prodan, Disordered topological insulators: a non-commutative geometry perspective, J. Phys. A: Math. Theor. **44**, 113001 (2011).